PTPN2 regulates T cell lineage commitment and αβ versus γδ specification

Florian Wiede,[1,2] Jarrod A. Dudakov,[3] Kun-Hui Lu,[1,2] Garron T. Dodd,[1,2] Tariq Butt,[1,2] Dale I. Godfrey,[4,5] Andreas Strasser,[6,7] Richard L. Boyd,[3] and Tony Tiganis[1,2,8]

[1]Monash Biomedicine Discovery Institute, [2]Department of Biochemistry and Molecular Biology, and [3]Department of Anatomy and Developmental Biology, Monash University, Clayton, Victoria, Australia
[4]Australian Research Council Centre of Excellence in Advanced Molecular Imaging, [5]Department of Microbiology and Immunology and Peter Doherty Institute for Infection and Immunity, and [6]Department of Medical Biology, University of Melbourne, Parkville, Victoria, Australia
[7]The Walter and Eliza Hall Institute of Medical Research, Parkville, Victoria, Australia
[8]Peter MacCallum Cancer Centre, Melbourne, Victoria, Australia

In the thymus, hematopoietic progenitors commit to the T cell lineage and undergo sequential differentiation to generate diverse T cell subsets, including major histocompatibility complex (MHC)–restricted αβ T cell receptor (TCR) T cells and non–MHC-restricted γδ TCR T cells. The factors controlling precursor commitment and their subsequent maturation and specification into αβ TCR versus γδ TCR T cells remain unclear. Here, we show that the tyrosine phosphatase PTPN2 attenuates STAT5 (signal transducer and activator of transcription 5) signaling to regulate T cell lineage commitment and SRC family kinase LCK and STAT5 signaling to regulate αβ TCR versus γδ TCR T cell development. Our findings identify PTPN2 as an important regulator of critical checkpoints that dictate the commitment of multipotent precursors to the T cell lineage and their subsequent maturation into αβ TCR or γδ TCR T cells.

The Journal of Experimental Medicine

INTRODUCTION

In the thymus, BM-derived T cell precursors undergo extensive proliferation and sequential differentiation to generate diverse T cell subsets, including MHC-restricted αβ TCR T cells, such as $CD4^+$ and $CD8^+$ T cells. The earliest progenitors are defined by their lack of cell surface TCRs and CD4 and CD8 coreceptors. These $CD4^-CD8^-$ double-negative (DN) thymocytes (also sometimes called $CD3^-CD4^-CD8^-$ triple negative) can be subdivided into four subsets (Godfrey et al., 1993). The DN1 ($c\text{-}KIT^+CD44^+CD25^-$) subset is heterogeneous and includes progenitors for the T cell, macrophage, dendritic cell, and NK cell lineages (Porritt et al., 2004; Carpenter and Bosselut, 2010; Rothenberg, 2011). DN1 cells differentiate into DN2 ($CD44^+CD25^+$) and undergo cellular expansion. Immediately before DN2 cells differentiate into DN3 cells ($CD44^-CD25^+$), early DN2 cells (DN2a) transition to an intermediate stage (DN2b) where they up-regulate T cell lineage genes and become irreversibly committed to the T cell lineage (Carpenter and Bosselut, 2010; Yui et al., 2010; Rothenberg, 2011; Zhang et al., 2012). The expression of the transcription factor BCL11b is essential for T cell lineage commitment, with *Bcl11b* deletion resulting in a profound developmental block at the DN2a stage (Ikawa et al., 2010; Li et al., 2010a). *Bcl11b* expression is first detected at the DN2a stage and increases as cells transition to the DN2b stage (Yui et al., 2010; Zhang et al., 2012; Kueh et al., 2016). Notch 1 signaling and Notch-activated transcription factors up-regulate and maintain *Bcl11b* expression and thereby establish and maintain T cell identity (Wakabayashi et al., 2003; Li et al., 2010b; Yui et al., 2010; Kueh et al., 2016). DN2a thymocyte survival and expansion depend on IL-7/IL-7 receptor-α (IL-7R-α) signaling via the JAK-1/3/STAT5 pathway to promote the expression of survival factors, such as BCL-2, and the expression of cell cycle regulators, such as cyclin D2 (Akashi et al., 1997; Maraskovsky et al., 1997; von Freeden-Jeffry et al., 1997; Yao et al., 2006). However, beyond affecting DN2a thymocyte survival and proliferation, the extent of STAT5 activation also dictates the differentiation of cells from the DN2a to the DN2b stage. In particular, the repression of IL-7/IL-7R/STAT5 tyrosine phosphorylation–dependent signaling is critical for the optimal induction of *Bcl11b* expression (Ikawa et al., 2010; Kueh et al., 2016). Precisely how IL-7/IL-7R signaling is reduced to influence T cell lineage specification in vivo remains un-

Correspondence to Tony Tiganis: Tony.Tiganis@monash.edu; Florian Wiede: Florian.Wiede@monash.edu

J.A. Dudakov's present address is Program in Immunology, Clinical Research Division, Fred Hutchinson Cancer Research Center, Seattle, WA.

R.L. Boyd's present address is Hudson Institute of Medical Research, Clayton, Victoria, Australia.

Abbreviations used: APC, allophycocyanin; D-PBS, Dulbecco-PBS; DN, double negative; DP, double positive; IEL, intraepithelial lymphocyte; LP, lamina propria; MFI, mean fluorescence intensity; MSCV, murine stem cell virus; PB, Pacific blue; PI3K, phosphatidylinositol 3-kinase; PTK, protein tyrosine kinase; PTP, protein tyrosine phosphatase; SFK, SRC family kinase; SP, single positive; WBM, whole BM.

The Rockefeller University Press
J. Exp. Med. 2017 Vol. 214 No. 9 2733–2758
https://doi.org/10.1084/jem.20161903

known. In part, this may involve a repression of IL-7R expression, as IL-7R is down-regulated as cells transition from DN2 to DN3 (Yu et al., 2004). Alternatively, this may occur by the repression of IL-7–induced and JAK-1/3–mediated STAT5 signaling by negative regulators, such as protein tyrosine phosphatases (PTPs).

At the DN3 stage, *Tcrβ*, *γ*, and *δ* gene rearrangements allow for the development of MHC-restricted αβ TCR T cells that play a central role in adaptive immunity and a smaller population of non-MHC–restricted γδ TCR T cells that display rapid innate-like, tissue-localized responses to microbial and nonmicrobial stresses to influence adaptive immunity (Hayday et al., 1985; Carpenter and Bosselut, 2010; Chien et al., 2014). DN3 cell commitment to the αβ TCR T cell lineage requires that a chromosomally rearranged and in-frame TCR-β pairs with the invariant pre–T-α chain to form the pre-TCR. The pre-TCR signals in a CD45-dependent manner (Byth et al., 1996) in the absence of ligand (Yamasaki et al., 2006) via the SRC family kinase (SFK) lymphocyte-specific protein tyrosine kinase (LCK; Molina et al., 1992) and canonical TCR-αβ/CD3 signaling intermediates that include the protein tyrosine kinases (PTKs) ζ chain–associated protein kinase 70 (ZAP-70) and spleen tyrosine kinase (SYK; Cheng et al., 1997). This is essential for DN3 thymocyte proliferation, survival, and maturation through to the DN4 ($CD44^-CD25^-$) stage and the expression of the CD4 and CD8 coreceptors to then form $CD4^+CD8^+$ double-positive (DP) cells. DN3 cells that lack in-frame *Tcrβ* gene arrangements and hence are unable to generate a pre-TCR signal are arrested in their differentiation and undergo cell death. This process is referred to as β selection and marks a critical checkpoint in TCR-αβ T cell development (Godfrey et al., 1993; Carpenter and Bosselut, 2010). To date, the regulation of β selection remains largely unexplored. Moreover, the processes that drive common DN3 precursors to develop into αβ TCR versus γδ TCR T cells are also not well understood. It is generally considered that strong TCR signaling favors γδ T cell commitment, whereas weaker pre-TCR signaling favors TCR-α gene rearrangement and the development of αβ T cells (Haks et al., 2005; Hayes et al., 2005; Kreslavsky et al., 2008; Zarin et al., 2015; Muñoz-Ruiz et al., 2016). Akin to pre-TCR signaling, TCR-γδ signaling is reliant on the SFKs LCK and FYN (Molina et al., 1992; Groves et al., 1996). Importantly, γδ T cell development is also reliant on IL-7–induced STAT5 signaling, which is necessary for TCR-γ gene rearrangement and expression (Cao et al., 1995; Maki et al., 1996; Moore et al., 1996; Kang et al., 1999, 2001; Ye et al., 1999, 2001).

Single nucleotide polymorphisms in the gene encoding the tyrosine phosphatase PTPN2 that result in decreased *PTPN2* mRNA in T cells have been linked to the development of inflammatory disorders and autoimmunity (Wellcome Trust Case Control Consortium, 2007; Todd et al., 2007; Smyth et al., 2008; Festen et al., 2011; Long et al., 2011). PTPN2 is a key negative regulator of TCR-αβ signaling, acting to dephosphorylate the SFKs LCK and FYN (Wiede et al., 2011), the most proximal tyrosine kinases activated by the TCR (Straus and Weiss, 1992; Iwashima et al., 1994; Palacios and Weiss, 2004). In peripheral T cells, PTPN2 sets the threshold for TCR-instigated responses by attenuating SFK signaling and preventing overt responses to low-affinity self-antigens in the context of antigen cross-presentation and T cell homeostasis (Wiede et al., 2011, 2012, 2014a,b). PTPN2 also negatively regulates cytokine signaling, dephosphorylating and inactivating the JAK-1 and -3 PTKs and STAT family members, including STAT1, STAT3, and STAT5 in a cell type– and context-dependent manner (Simoncic et al., 2002; ten Hoeve et al., 2002; Fukushima et al., 2010; Loh et al., 2011; Wiede et al., 2011, 2014b, 2017; Gurzov et al., 2014; Spalinger et al., 2015). In particular, PTPN2 attenuates IL-2/STAT5 signaling in activated $CD4^+$ and $CD8^+$ T cells to repress their expansion as well as cytotoxic T cell differentiation (Wiede et al., 2011, 2014b). Furthermore, PTPN2 attenuates IL-21/STAT3 signaling and $CD4^+$ T cell expansion and the generation of T follicular helper cells (Wiede et al., 2017). $Ptpn2^{-/-}$ (C57BL/6) mice succumb to wasting disease by 3–5 wk of age, accompanied by the infiltration of immune cells into nonlymphoid tissues, thymic atrophy, and defects in hematopoeisis, especially in BM B cell and erythroid development (You-Ten et al., 1997; Wiede et al., 2012). Interestingly, at 2 wk of age, $Ptpn2^{-/-}$ (C57BL/6) mice are growth retarded, but otherwise appear and behave normally. At this stage, *Ptpn2* deficiency results in increased thymocyte development and enhanced positive selection (Wiede et al., 2012). This is also seen in *Lck*-Cre;$Ptpn2^{fl/fl}$ mice where *Ptpn2* is specifically deleted in thymocytes and T cells (Wiede et al., 2011), consistent with the influence being cell autonomous and PTPN2 directly influencing thymic T cell development. Herein, we have explored the role of PTPN2 in the regulation of SFK and STAT5 signaling in T cell lineage commitment and αβ TCR versus γδ TCR T cell specification.

RESULTS

DN thymocyte development is altered in PTPN2-deficient mice

We assessed the impact of PTPN2 deficiency on DN thymocyte development (Fig. S1, A and B; gating strategy) in 14–16-d-old $Ptpn2^{-/-}$ (C57BL/6) mice, before the onset of the overt morbidity that otherwise occurs between 3 and 5 wk of age (Wiede et al., 2012). In thymi from $Ptpn2^{-/-}$ mice, lineage marker negative c-KIT^+ DN1 cell numbers were unaltered, whereas DN2–4 cells were increased, consistent with enhanced DN thymocyte development (Fig. 1 A). We also assessed the impact of PTPN2 deletion in adult mice by generating *Ptpn2*-floxed mice that also contained the *Mx1-Cre* transgene (Cre recombinase under the control of the type 1 interferon inducible promoter; Kühn et al., 1995) and the *Rosa26-loxP-stop-loxP-YFP* reporter to facilitate the conditional deletion of PTPN2 upon administration of poly (I:C). Using this approach, we achieved 86% recombination, as assessed by YFP (reporter for CRE activity) fluorescence, and

82% PTPN2 deletion, as assessed by flow cytometry in YFP^+ DN thymocytes (Fig. S2). After 4 wk of PTPN2 deletion, *Mx1*-Cre;*Ptpn2*$^{fl/fl}$ (C57BL/6) mice had increased circulating inflammatory cytokines, an effector/memory T cell phenotype, and increased T follicular helper and B cell development (Wiede et al., 2017). Nonetheless, PTPN2 deletion in adult *Mx1*-Cre;*Ptpn2*$^{fl/fl}$ mice did not cause any significant change in lineage-negative (Lin^-) c-KIT^+ DN1 cells but resulted in increased DN2–4 cells (Fig. 1 B). The increase in DN thymocytes in poly (I:C)–treated *Mx1*-Cre;*Ptpn2*$^{fl/fl}$ mice was accompanied by an increase in DP cells and thereon increased numbers of single-positive (SP) $CD4^+CD8^-$ and $CD4^-CD8^+$ thymocytes (Fig. S3 A). As noted previously in *Ptpn2*$^{-/-}$ and *Lck*-Cre;*Ptpn2*$^{fl/fl}$ mice (Wiede et al., 2011, 2012), PTPN2 deletion in *Mx1*-Cre;*Ptpn2*$^{fl/fl}$ mice was accompanied by increased positive selection (as assessed by CD69 and TCR-β expression; Fig. S3 A). The capacity of PTPN2 deficiency to enhance DN2–4 development was also evident when either whole BM (WBM) cells (Fig. S3 B), purified Lin^- c-KIT^{hi} SCA-1^{hi} BM cells (Fig. S3 C), or purified Lin^- c-KIT^{hi} DN1 thymocytes (Fig. 1 C) from *Ptpn2*$^{+/+}$ versus *Ptpn2*$^{-/-}$ mice were cultured on OP9 stromal cells expressing the Notch 1 ligand, Delta-like 1 (DL1), in the presence of FMS-like tyrosine kinase 3 ligand (FLT3L) and IL-7 (Fig. 1 C). The OP9-DL1 co-culture model also allows for DN thymocytes to develop into DP thymocytes and thereon into immature $CD24^{hi}$TCR-$β^-$ SP thymocytes ex vivo (Schmitt and Zúñiga-Pflücker, 2002; Schmitt et al., 2004). We found that PTPN2-deficient c-KIT^{hi} DN1 thymocytes cultured with OP9-DL1 cells in the presence of FLT3L and IL-7 also yielded increased DP thymocytes and immature $CD24^{hi}$TCR-$β^-$ SP thymocytes compared with cultures of control DN1 thymocytes (Fig. 1 C and Fig. S3 D). These results are consistent with PTPN2 eliciting cell-intrinsic effects on thymocyte development.

PTPN2 regulates STAT5 signaling in DN thymocytes

IL-7/IL-7R signaling has a critical role during early T cell development, promoting DN cell survival, proliferation, and differentiation. IL-7 signals via IL-7R-α and the common γ chain to the tyrosine kinases JAK-1 and -3 to phosphorylate STAT5, and this mediates, among other processes, the expression of the antiapoptotic protein BCL-2 to promote thymocyte survival (Akashi et al., 1997; Maraskovsky et al., 1997; von Freeden-Jeffry et al., 1997; Yao et al., 2006). Indeed, defects in thymic T cell development in IL-7– or IL-7R-α–deficient mice can be rescued by transgenic overexpression of BCL-2 (Akashi et al., 1997; Maraskovsky et al., 1997). PTPN2 has the capacity to antagonize cytokine receptor signaling, including IL-7/IL-7R signaling, through the dephosphorylation of JAK-1/3 and STAT5 (Simoncic et al., 2002; Gurzov et al., 2014). We found that STAT5 Y694 phosphorylation (p-STAT5), a marker of STAT5 activation, was increased in DN thymocytes from 14-d-old *Ptpn2*$^{-/-}$ mice compared with their WT counterparts (Fig. 1 D). In particular, p-STAT5 was increased by approximately four- to fivefold at the DN2a and DN2b stages and to a lesser extent at other stages of thymocyte development (Fig. 1 D). p-STAT5 was also elevated in DN2 and DN3 thymocytes from poly (I:C)–treated *Mx1*-Cre;*Ptpn2*$^{fl/fl}$ mice compared with those from control animals (Fig. S4 A) and in DN2/3 thymocytes generated ex vivo when WBM cells (Fig. 1 E) or Lin^-c-KIT^{hi}SCA-1^{hi} BM cells (Fig. 1 F) from *Ptpn2*$^{-/-}$ mice were cultured on OP9-DL1 stromal cells. The increase in STAT5 activation occurred independently of increases in the expression of the cell surface receptors for IL-7 (CD127) and IL-2 (CD25/CD132; Fig. S4 B) or overt changes in JAK-1 Y1022/Y1023 phosphorylation (Fig. 1 F), a marker of JAK-1 activation. This is in keeping with PTPN2 acting directly on STAT5. The increase in p-STAT5 caused by the loss of PTPN2 was accompanied by the increased expression of BCL-2 (Fig. 1, D and G; and Fig. S4 A) and, albeit to a lesser extent, MCL-1 (Fig. 1 G), another antiapoptotic BCL-2 family member that is also critical for thymocyte survival (Opferman et al., 2003; Campbell et al., 2012). In keeping with the heightened expression of prosurvival BCL-2 family members, we found that *Ptpn2*$^{-/-}$ DN thymocytes exhibited increased resistance to dexamethasone in vitro compared with their WT counterparts (Fig. S4 C). The increase in STAT5 activation in *Ptpn2*$^{-/-}$ DN2 cells in vivo was also accompanied by increased DN2a proliferation, as assessed by Ki67 staining (Fig. 1 H). The increased DN2a proliferation was also evident when FACS-sorted DN2a cells were cultured on OP9-DL1 stromal cells (Fig. 2 F). However, loss of PTPN2 had no impact on the proliferation of DN2b, DN3, and DN4 cells in vivo (Fig. 1 H). These results indicate that PTPN2 negatively regulates STAT5 signaling, DN2/3 thymocyte survival, and DN2a proliferation.

PTPN2 deficiency represses T cell lineage commitment

To begin to understand the role of PTPN2 in DN thymocyte development, we sought to dissect the impact of its loss at critical developmental checkpoints. DN thymocytes become committed to the T cell lineage after the DN2 stage. Before this stage, c-KIT^{hi} DN1 and early c-KIT^{hi} DN2 cells (DN2a) undergo self-renewal and retain the potential to differentiate into other hematopoietic lineages, in particular dendritic and NK cells (Porritt et al., 2004; Rothenberg, 2011). As proliferation slows, DN2a cells transition into an intermediate c-KIT^{lo} DN2 stage (DN2b), where they become irreversibly committed to the T cell lineage, and thereon differentiate into DN3 thymocytes and beyond (Carpenter and Bosselut, 2010; Rothenberg, 2011). We found that PTPN2 deficiency increased the number of DN2a but not that of DN2b cells in 14-d-old *Ptpn2*$^{-/-}$ mice (Fig. 2 A). This suggests that PTPN2 deficiency may promote DN2a cell expansion while repressing the DN2a to DN2b transition. Although one may expect that DN2b cells would be diminished as a consequence of such defective transition, this may be countered by the increased STAT5 signaling (Fig. 1, D–F) and the consequently increased expression of the prosurvival proteins BCL-2 and MCL-1, which is also evident in DN2b cells (Fig. 1 G). This

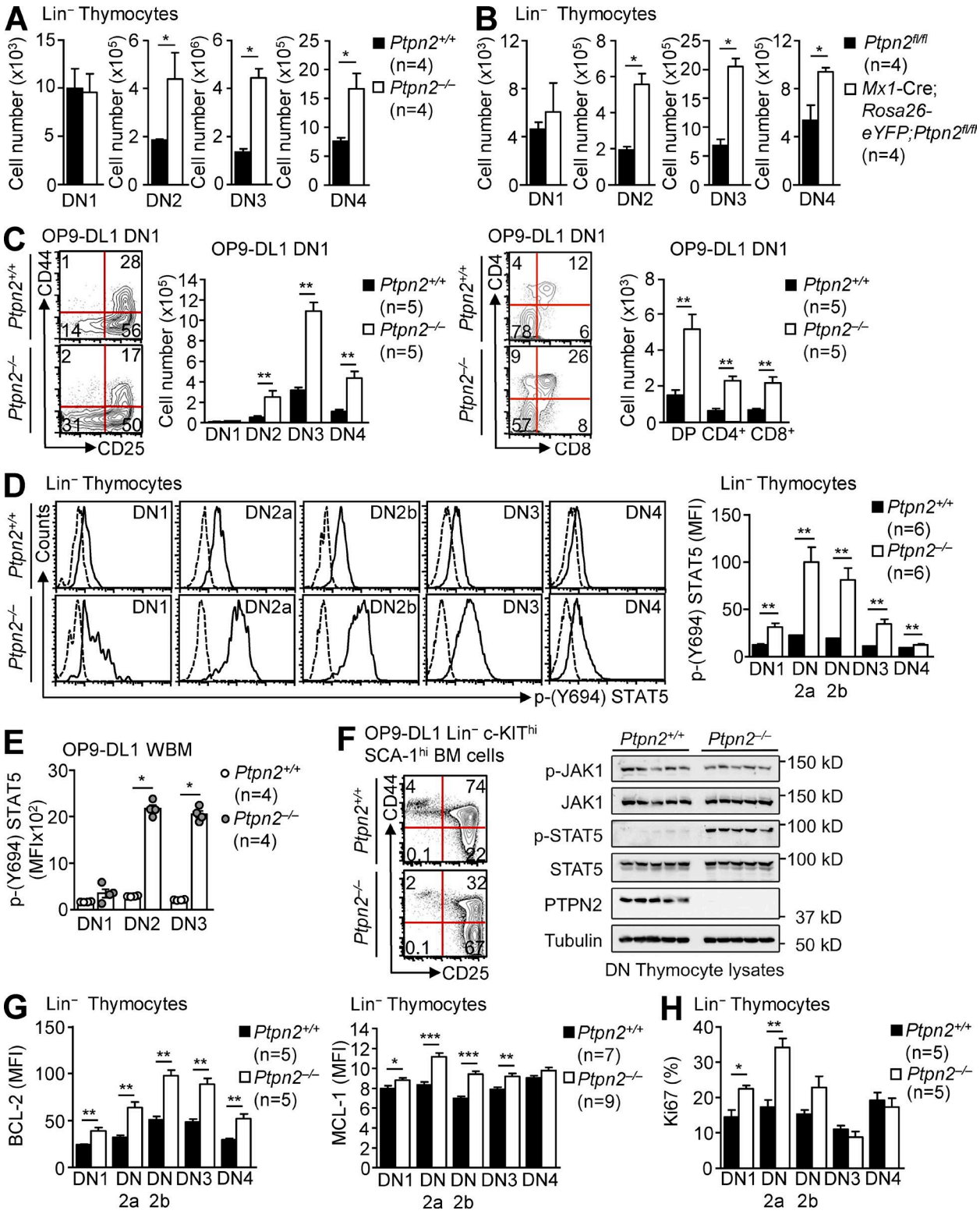

Figure 1. **PTPN2 deficiency influences thymocyte differentiation and increases STAT5 signaling.** (A and B) Lineage (Lin)$^-$ thymocytes from *Ptpn2*$^{+/+}$ (C57BL/6) and *Ptpn2*$^{-/-}$ (C57BL/6) mice (A) and poly (I:C)–treated *Rosa26-eYFP;Ptpn2*$^{fl/fl}$ (C57BL/6) or *Mx1*-Cre;*Rosa26-eYFP;Ptpn2*$^{fl/fl}$ (C57BL/6) mice (B) were stained with fluorochrome-conjugated antibodies against CD25, CD44, and c-KIT, and CD4/CD8 (DN) cell subsets were quantified by flow cytometry. (C) FACS-purified DN1 thymocytes from *Ptpn2*$^{+/+}$ (C57BL/6) and *Ptpn2*$^{-/-}$ (C57BL/6) mice were cultured for 10 d on OP9-DL1 stromal cells and stained for CD25, CD44, CD4, and CD8, and DN cell subsets were quantified by flow cytometry. (D, G, and H) Lin$^-$ thymocytes from *Ptpn2*$^{+/+}$ (C57BL/6) and *Ptpn2*$^{-/-}$ (C57BL/6)

would be consistent with studies demonstrating that IL-7/IL-7R-α–induced STAT5 signaling promotes the survival of DN2 cells via induction of BCL-2 expression (Akashi et al., 1997; Maraskovsky et al., 1997; von Freeden-Jeffry et al., 1997; Yao et al., 2006).

The impact of PTPN2 deficiency on DN thymocyte development and lineage commitment in *Ptpn2*$^{-/-}$ (C57BL/6) mice or poly (I:C)–treated *Mx1*-Cre;*Ptpn2*$^{fl/fl}$ (C57BL/6) mice may be thymocyte intrinsic, or it could conversely be associated with alterations in the thymic stroma (in which PTPN2 is also lost) or the overall inflammatory environment in which the DN thymocytes develop. To discriminate between these possibilities, we generated BM chimeras by the cotransfer of WBM cells from BALB/c Thy1.1$^+$ WT mice with BALB/c Thy1.2$^+$ *Ptpn2*$^{+/+}$ or *Ptpn2*$^{-/-}$ mice into lethally irradiated BALB/c Thy1.2$^+$ WT hosts (Fig. 2 B). We assessed the capacity of Thy1.2$^+$ *Ptpn2*$^{+/+}$ or Thy1.2$^+$ *Ptpn2*$^{-/-}$ T cell progenitors to compete with their congenic Thy1.1$^+$ WT counterparts in the chimeric mice by examining T cell development after 7 wk. We found that PTPN2 deficiency had no effect on the number of c-KIT$^+$ CD44$^+$CD25$^-$ DN1 cells but increased DN2a cells, but not DN2b cells (Fig. 2, C and D), as already observed in 14-d-old *Ptpn2*$^{-/-}$ mice (Fig. 2 A) or poly (I:C)–treated *Mx1*-Cre; *Ptpn2*$^{fl/fl}$ (C57BL/6) mice (Fig. 5 A). Similar results were seen when WBM from C57BL/6 Ly5.1$^+$ mice was cotransferred with that of C57BL/6 Ly5.2$^+$ *Ptpn2*$^{+/+}$ or *Ptpn2*$^{-/-}$ animals into lethally irradiated C57BL/6 Ly5.1/2$^+$ congenic WT hosts (Fig. S3, E–G). These results are consistent with PTPN2 eliciting cell-intrinsic effects to regulate T cell lineage commitment. Importantly, PTPN2 deficiency also resulted in increased DN3 and DN4 cells and thereon increased the numbers of DP and SP thymocytes (Fig. S3 H). Therefore, beyond influencing T cell lineage commitment, PTPN2 deficiency may increase progression at the DN3 stage independent of its effects on DN2 thymocytes.

To further explore the impact of PTPN2 deficiency on T cell lineage commitment, we sorted single DN2a *Ptpn2*$^{+/+}$ versus *Ptpn2*$^{-/-}$ cells into a 96-well plate coated with OP9-DL1 cells in the presence of FLT3L and IL-7 and assessed DN2a expansion and differentiation into DN2b cells, thereby testing for commitment to the T cell lineage (Fig. 2, E and F). PTPN2 deficiency significantly increased the number of DN2a cells (Fig. 2 E), and this was accompanied by increased cell proliferation, as monitored by staining for Ki67 (Fig. 2 F). PTPN2 deficiency also increased the expression of the antiapoptotic protein BCL-2 (Fig. 2 F), in keeping with enhanced cell survival. Importantly, despite the increased DN2a cell expansion, we found that DN2b cells were not increased numerically (Fig. 2 E). To determine whether the transition to the DN2b stage and thereby T cell lineage commitment may be defective, we examined whether the accumulation of PTPN2-deficient DN2a cells may be accompanied by the increased generation of non–T cell lineage derivatives, including Lin$^-$CD11c$^+$ dendritic and Lin$^-$NK1.1$^+$ NK cells. To this end, we compared the fate of DN2a cells cultured on OP9 stromal cells that lacked DL1 and did not support progression to the DN2b stage but promoted alternate lineage fates (Porritt et al., 2004) with those cultured on OP9-DL1 cells in the presence of FLT3L and IL-7, a condition that does support further T cell differentiation (Fig. 2, G and H; and Fig. S4, D and E). We found that PTPN2 deficiency further enhanced the generation of Lin$^-$CD11c$^+$ and Lin$^-$NK1.1$^+$ cells when DN2a cells were co-cultured with OP9 cells. Importantly, PTPN2 deficiency even allowed the generation of Lin$^-$CD11c$^+$ and Lin$^-$NK1.1$^+$ cells when DN2a cells were co-cultured with OP9-DL1 cells, a condition under which CD11c$^+$ and NK1.1$^+$ cells otherwise are only rarely produced (Fig. 2, G and H). These results are consistent with PTPN2 deficiency perturbing T cell lineage commitment so that accumulated DN2a cells are diverted into non–T cell lineage fates. To further explore this, we also assessed the impact of PTPN2 deficiency on *Bcl11b* expression, which previous studies have shown is repressed by heightened STAT5 signaling to repress the DN2a to DN2b transition (Ikawa et al., 2010; Li et al., 2010a). We found that the increase in *Bcl11b* gene expression that was evident in WT cells that had transitioned from the DN2a to the DN2b stage was repressed by PTPN2 deficiency (Fig. 2 I). Collectively, these results indicate that PTPN2 deficiency promotes the proliferation and survival of DN2 cells while also repressing their transition into the DN2b stage and thus their commitment to the T cell lineage.

PTPN2 regulates STAT5-dependent DN thymocyte development

To determine the extent to which the elevated STAT5 signaling might contribute to the alterations in DN thymocyte development, we adopted genetic and pharmaco-

mice were stained for CD25, CD44, and c-KIT and either intracellular p-(Y694) STAT5 (p-STAT5) (D), intracellular BCL-2 and MCL-1 (G), or the cell proliferation marker Ki67 (H) were determined in DN subsets by flow cytometry. (E) WBM cells from *Ptpn2*$^{+/+}$ (C57BL/6) and *Ptpn2*$^{-/-}$ (C57BL/6) mice were cultured on OP9-DL1 stromal cells for 9 d. Lin$^-$ thymocytes were harvested and stained for CD25, CD44, and intracellular p-(Y694) STAT5 (p-STAT5). The mean fluorescence intensities (MFIs) for intracellular staining of p-STAT5 was determined by flow cytometry. (F) FACS-purified Lin$^-$c-KIT^{hi}SCA-1^{hi} BM cells from individual *Ptpn2*$^{+/+}$ (C57BL/6) (n = 5) and *Ptpn2*$^{-/-}$ (C57BL/6) (n = 5) mice were cultured on OP9-DL1 stromal cells for 9 d. DN2/3 thymocytes were harvested and stained for CD25 and CD44, and DN subsets were determined by flow cytometry. DN2/3 thymocyte lysates were resolved by SDS-PAGE and immunoblotted for p-STAT, STAT5, p-(Y1022/1023) JAK-1 (p-JAK1), JAK-1, PTPN2, and tubulin. Representative results (means ± SEM; *Ptpn2*$^{+/+}$, n = 4–7; *Ptpn2*$^{-/-}$, n = 4–9; *Rosa26-eYFP*;*Ptpn2*$^{fl/fl}$, n = 4; *Mx1*-Cre;*Rosa26-eYFP*;*Ptpn2*$^{fl/fl}$, n = 4) and representative cytometry profiles (C, D, and F) and immunoblots (F) from at least two independent experiments are shown. In F, each lane represents the cell lysate from one individual mouse. Significance was determined using two-tailed Mann-Whitney U test; *, $P < 0.05$; **, $P < 0.01$; ***, $P < 0.001$.

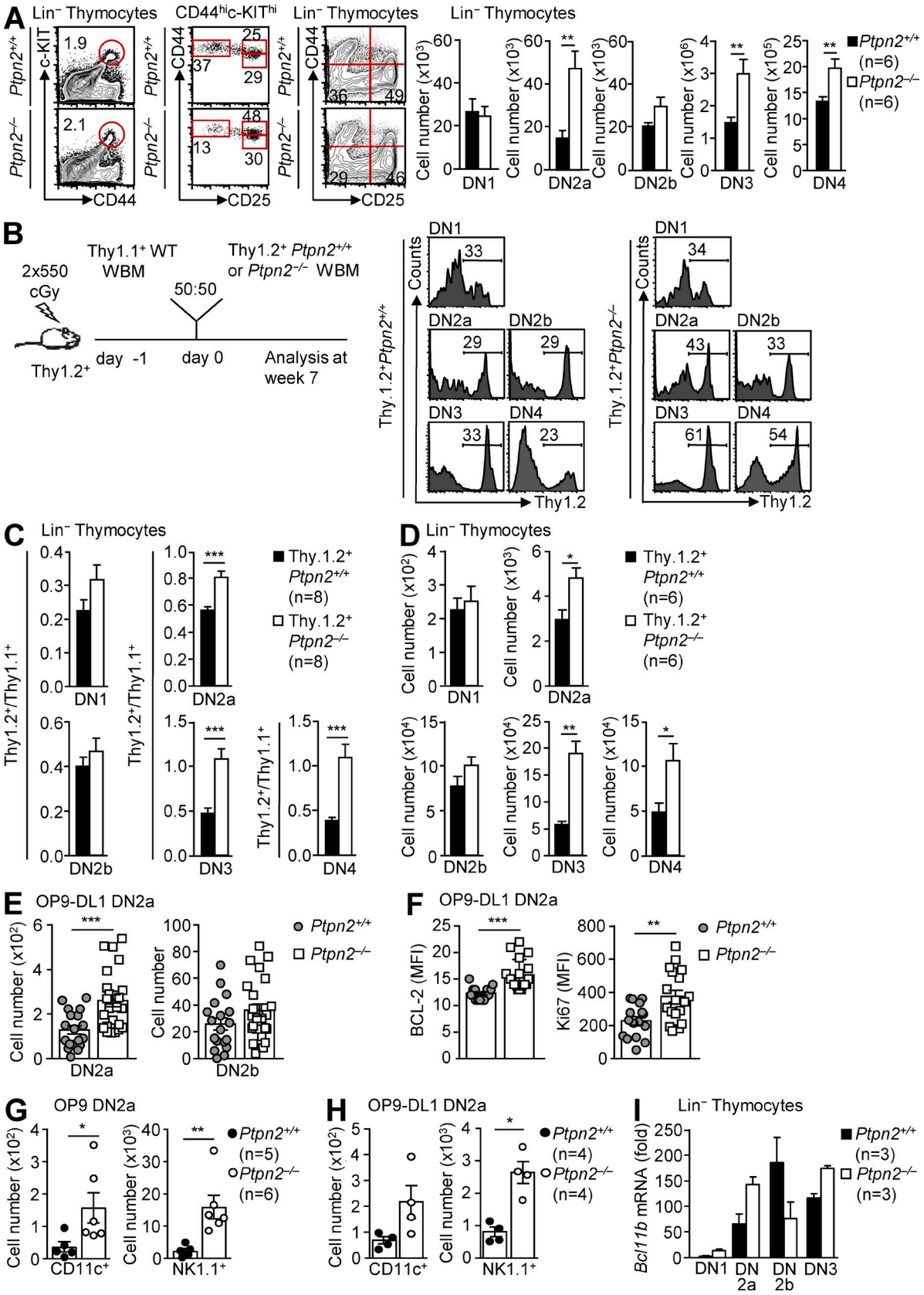
A
Lin⁻ Thymocytes
CD44hic-KIThi
Lin⁻ Thymocytes
Lin⁻ Thymocytes
Ptpn2+/+
Ptpn2−/−
c-KIT
CD44
CD25
1.9
2.1
25
37
29
48
13
30
36
49
29
46
Cell number (x10³)
Cell number (x10⁶)
Cell number (x10⁵)
DN1
DN2a
DN2b
DN3
DN4
**
Ptpn2+/+ (n=6)
Ptpn2−/− (n=6)
B
Thy1.1+ WT WBM
Thy1.2+ Ptpn2+/+ or Ptpn2−/− WBM
2x550 cGy
50:50
Thy1.2+
day -1
day 0
Analysis at week 7
Thy.1.2+Ptpn2+/+
Thy.1.2+Ptpn2−/−
Counts
Thy1.2
33
29
29
33
23
34
43
33
61
54
C
Lin⁻ Thymocytes
Thy1.2+/Thy1.1+
DN1
DN2a
DN2b
DN3
DN4
***
Thy.1.2+ Ptpn2+/+ (n=8)
Thy.1.2+ Ptpn2−/− (n=8)
D
Lin⁻ Thymocytes
Cell number (x10²)
Cell number (x10³)
Cell number (x10⁴)
*
**
Thy.1.2+ Ptpn2+/+ (n=6)
Thy.1.2+ Ptpn2−/− (n=6)
E
OP9-DL1 DN2a
Cell number (x10²)
Cell number
DN2a
DN2b
***
Ptpn2+/+
Ptpn2−/−
F
OP9-DL1 DN2a
BCL-2 (MFI)
Ki67 (MFI)
***
**
Ptpn2+/+
Ptpn2−/−
G
OP9 DN2a
Cell number (x10²)
Cell number (x10³)
CD11c+
NK1.1+
*
**
Ptpn2+/+ (n=5)
Ptpn2−/− (n=6)
H
OP9-DL1 DN2a
Cell number (x10²)
Cell number (x10³)
CD11c+
NK1.1+
*
Ptpn2+/+ (n=4)
Ptpn2−/− (n=4)
I
Lin⁻ Thymocytes
Bcl11b mRNA (fold)
DN1
DN 2a
DN 2b
DN3
Ptpn2+/+ (n=3)
Ptpn2−/− (n=3)

logical approaches to correct the enhanced STAT5 signaling. To this end, we first assessed the impact of superimposing STAT5 deficiency on *Mx1*-Cre;*Ptpn2*$^{fl/fl}$ mice. We crossed *Mx1*-Cre;*Ptpn2*$^{fl/fl}$ mice onto a *Stat5*$^{fl/+}$ (Cui et al., 2007) background (generating *Mx1*-Cre;*Ptpn2*$^{fl/fl}$;*Stat5*$^{fl/+}$ mice) and treated these animals with poly (I:C) to reduce STAT5 levels in PTPN2-deleted cells by 50%. *Stat5* heterozygosity reduced the numbers of DN2, DN3, and DN4 cells to the levels seen in control (WT) animals (Fig. 3 A). To examine whether the impact of *Stat5* heterozygosity on DN thymocyte development might be cell autonomous, we tested the consequences of genetically reducing STAT5 protein levels or pharmacologically inactivating JAK/STAT5 signaling on DN thymocyte development in culture. For this, we cultured WBM cells from poly (I:C)–treated *Ptpn2*$^{fl/fl}$, *Mx1*-Cre; *Ptpn2*$^{fl/fl}$, or *Mx1*-Cre;*Ptpn2*$^{fl/fl}$;*Stat5*$^{fl/+}$ mice on OP9-DL1 stromal cells (Fig. 3 B) or cultured WBM cells from *Ptpn2*$^{+/+}$ or *Ptpn2*$^{-/-}$ mice on OP9-DL1 cells in the presence or absence of the JAK inhibitor CMP6 and assessed DN thymocyte development (Fig. 3 C). Notably, *Stat5* heterozygosity (Fig. 3 B) or the inhibition of JAK PTKs (Fig. 3 C), with the consequent repression of p-STAT5 levels to those in control cells, significantly reduced the numbers of DN2 and DN3 cells (Fig. 3, B and C; and Fig. S4, F and G). Collectively, these results demonstrate that PTPN2 deficiency impacts on DN thymocyte development through the attenuation of STAT5 signaling.

The effects of PTPN2 on DN thymocyte development and STAT5 signaling might be mediated directly via the dephosphorylation of STAT5 and/or indirectly via the dephosphorylation of JAK PTKs, or may even be independent of PTPN2 phosphatase activity. The 45-kD form of PTPN2 that predominates in T cells shuttles between the nucleus, where it dephosphorylates STAT family members, and the cytoplasm, where it dephosphorylates cytoplasmic tyrosyl-phosphorylated substrates, such as JAK-1/3 and SFKs (Simoncic et al., 2002; ten Hoeve et al., 2002; van Vliet et al., 2005; Tiganis and Bennett, 2007; Loh et al., 2011). The 45-kD PTPN2 protein is actively transported to the nucleus by a bipartite nuclear localization sequence (Tiganis et al., 1997) but passively diffuses out of the nucleus (Lam et al., 2001). We have shown previously that fusing GFP to 45-kD PTPN2 prevents exit from the nucleus (Lam et al., 2001), as its mass (72 kD) exceeds the diffusion limits of the nuclear pore complex (Nigg, 1997). Therefore, to determine whether PTPN2 may elicit its effects on DN thymocyte development through the dephosphorylation of STAT5 in the nucleus or cytoplasmic PTKs, such as JAK-1/3, we assessed the impact of overexpressed WT or catalytically inactive PTPN2 versus GFP-PTPN2 on this process. WBM cells from C57BL/6 mice were transduced with mCherry-expressing control retroviruses or ones encoding WT PTPN2, catalytically inactive PTPN2-R222M, or exclusively nuclear GFP-PTPN2 and then transplanted into lethally irradiated congenic hosts. DN thymocyte development in recipient animals was assessed after 7 wk (Fig. 4). The WT PTPN2 was overexpressed by approximately twofold over the endogenous PTPN2, and this decreased the numbers of c-KIT^{hi}CD44^{+}CD25^{-} DN1 cells by 30% (Fig. 4 B). The decrease in DN1 cells might have been caused by a direct effect on the DN1 cells themselves or by an effect on more immature BM progenitors, given that PTPN2 has been implicated in hematopoietic stem cell expansion (You-Ten et al., 1997; Bourdeau et al., 2013). Regardless, PTPN2 overexpression resulted in yet a further reduction in the number of DN2 cells and their progression into DN3 and DN4 (Fig. 4 B). In contrast, the catalytically inactive PTPN2-R222M had no measurable impact on DN thymocyte development (Fig. 4 C). Finally, the GFP-PTPN2 fusion protein that was restricted to the nucleus in DN thymocytes (not depicted) was able to reduce the number of DN2 cells (Fig. 4 B). PTPN2- and GFP-PTPN2–repressed p-STAT5, but not p-JAK-1, in DN2/3 thymocytes derived from transduced Lin^{-} c-KIT^{hi} SCA-1^{hi} BM cells that had been allowed to differentiate on OP9-DL1 cells in culture (Fig. S4 H). Together, these findings indicate that PTPN2 can exert effects on DN thymocyte development through the dephosphorylation of STAT5 in the nucleus.

Figure 2. **PTPN2 deficiency represses T cell lineage commitment.** (A) Lin^{-} thymocytes from *Ptpn2*$^{+/+}$ (C57BL/6) and *Ptpn2*$^{-/-}$ (C57BL/6) mice were stained for CD25, CD44, and c-KIT, and DN cell subsets were quantified by flow cytometry. (B–D) Equal numbers of donor WBM cells (2×10^6) from Thy1.2^{+}*Ptpn2*$^{+/+}$ (BALB/c) or Thy1.2^{+}*Ptpn2*$^{-/-}$ (BALB/c) mice and congenic Thy1.1^{+} (BALB/c) competitor cells were transferred into lethally irradiated (2×550 cGy) BALB/c recipient animals. Donor cell contribution in the thymus was assessed at 7 wk after transplantation. (B) Representative FACS profiles showing percent donor (Thy1.2)-derived DN thymocyte subset reconstitution. (C) Donor Thy1.2^{+}*Ptpn2*$^{+/+}$ (BALB/c) or Thy1.2^{+}*Ptpn2*$^{-/-}$ (BALB/c) cells and Thy1.1^{+} competitor (BALB/c) DN subset ratios. (D) Absolute numbers of donor Thy1.2^{+}*Ptpn2*$^{+/+}$ (BALB/c) versus Thy1.2^{+}*Ptpn2*$^{-/-}$ (BALB/c) DN subsets. (E and F) DN2a thymocytes from *Ptpn2*$^{+/+}$ (C57BL/6) and *Ptpn2*$^{-/-}$ (C57BL/6) mice were single-cell sorted, cultured on OP9-DL1 stromal cells for 72 h, and then stained with fluorochrome-conjugated antibodies against CD25 and c-KIT. DN2a and DN2b cells were quantified by flow cytometry (E), and intracellular BCL-2 and Ki67 MFIs in DN2 cells were determined (F). (G and H) 10^2 DN2a thymocytes from *Ptpn2*$^{+/+}$ (C57BL/6) and *Ptpn2*$^{-/-}$ (C57BL/6) mice were FACS purified, cultured on OP9 (G) or OP9-DL1 (H) stromal cells for 5 d, and then stained with fluorochrome-conjugated antibodies against Lin markers, CD11c, and NK1.1. Cell subsets were quantified by flow cytometry. (I) *Bcl11b* mRNA levels in *Ptpn2*$^{+/+}$ (C57BL/6) and *Ptpn2*$^{-/-}$ (C57BL/6) DN thymocyte subsets were assessed by quantitative RT-PCR. Representative results (means ± SEM; *Ptpn2*$^{+/+}$, $n = 3$–6; *Ptpn2*$^{-/-}$, $n = 3$–6; Thy1.2^{+}.*Ptpn2*$^{+/+}$, $n = 6$–8; and Thy1.2^{+}.*Ptpn2*$^{-/-}$, $n = 6$–8) and representative cytometry profiles (A and B) from at least three independent experiments are shown. In E and F, pooled data from three independent experiments are shown. In A, C, D, G, and H, significance was determined using two-tailed Mann-Whitney *U* test; *, $P < 0.05$; **, $P < 0.01$; ***, $P < 0.001$. In E and F, significance was determined using two-tailed Student's *t* test. **, $P < 0.01$; ***, $P < 0.001$.

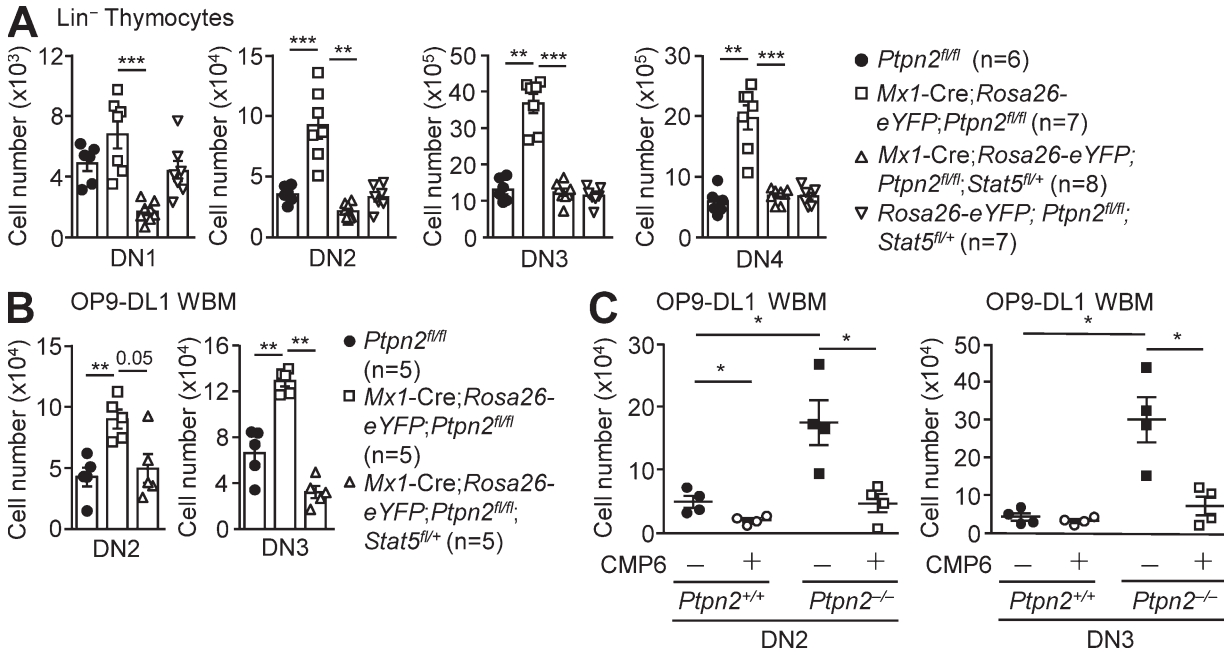

Figure 3. **STAT5 heterozygosity versus JAK PTK inhibition corrects DN thymocyte development associated with PTPN2 deficiency.** (A) Lin⁻ thymocytes from poly (I:C)–treated *Rosa26-YFP;Ptpn2*$^{fl/fl}$ (C57BL/6), *Mx1*-Cre;*Rosa26-eYFP;Ptpn2*$^{fl/fl}$;*Stat5*$^{+/-}$ (C57BL/6), *Mx1*-Cre;*Rosa26-eYFP;Ptpn2*$^{fl/fl}$ (C57BL/6), and *Rosa26-eYFP;Ptpn2*$^{fl/fl}$;*Stat5*$^{+/-}$ (C57BL/6) mice were stained for CD25, CD44, and c-KIT, and DN cell subsets were quantified by flow cytometry. (B) WBM cells from *Rosa26-eYFP;Ptpn2*$^{fl/fl}$ (C57BL/6), *Mx1*-Cre;*Rosa26-eYFP;Ptpn2*$^{fl/fl}$(C57BL/6);*Stat5*$^{+/-}$ (C57BL/6), and *Mx1*-Cre;*Rosa26-eYFP;Ptpn2*$^{fl/fl}$ (C57BL/6) mice were cultured on OP9-DL1 stromal cells. Lin⁻ thymocytes were harvested after 10 d and stained for CD25 and CD44, and DN cell subsets were quantified by flow cytometry. (C) WBM cells from *Ptpn2*$^{+/+}$ (C57BL/6) and *Ptpn2*$^{-/-}$ (C57BL/6) mice were cultured on OP9-DL1 stromal cells in the presence of the JAK PTK inhibitor CMP6 or vehicle control (DMSO). DN2 and DN3 cell numbers were quantified by flow cytometry. Representative results (means ± SEM; *Ptpn2*$^{+/+}$, *n* = 4; *Ptpn2*$^{-/-}$, *n* = 4; *Rosa26-eYFP;Ptpn2*$^{fl/fl}$, *n* = 5–6; *Mx1*-Cre;*Rosa26-eYFP;Ptpn2*$^{fl/fl}$, *n* = 5–7; *Mx1*-Cre;*Rosa26-eYFP;Ptpn2*$^{fl/fl}$;*STAT5*$^{fl/+}$, *n* = 5–8; and *Rosa26-eYFP;Ptpn2*$^{fl/fl}$;*STAT5*$^{fl/+}$, *n* = 7) from at least three independent experiments are shown. Significance was determined using two-tailed Mann-Whitney *U* test. *, P < 0.05; **, P < 0.01; ***, P < 0.001.

PTPN2 regulates STAT5-dependent T cell lineage commitment

Despite the critical role of IL-7/IL-7R signaling in DN2 cell survival and proliferation (Maraskovsky et al., 1996, 1997; Akashi et al., 1997; von Freeden-Jeffry et al., 1997), the repression of this pathway is thought to be necessary for BCL11b expression and hence the transition of cells from the DN2a stage to the DN2b stage with consequent T cell lineage commitment (Ikawa et al., 2010; Li et al., 2010a; Kueh et al., 2016). The molecular basis for the repression of IL-7/IL-7R signaling at this development checkpoint remains unknown. Our studies indicate that *Bcl11b* expression is decreased, T cell lineage commitment is repressed, and p-STAT5 is increased in DN2a/DN2b cells in the absence of PTPN2. Accordingly, we reasoned that PTPN2 deficiency may repress the transition from DN2a to DN2b and thereby favor the generation of alternate cell lineages by increasing STAT5 signaling. To test this, we determined whether attenuating STAT5 signaling in *Ptpn2*$^{-/-}$ DN2a thymocytes could alleviate the otherwise repressed T cell lineage commitment. To this end, we used a genetic approach and compared the DN2a and DN2b cell numbers between poly (I:C)–treated *Ptpn2*$^{fl/fl}$, *Mx1*-Cre;*Ptpn2*$^{fl/fl}$, and *Mx1*-Cre;*Ptpn2*$^{fl/fl}$;*Stat5*$^{fl/+}$ mice (Fig. 5 A). In addition, we cultured purified DN2a cells from poly (I:C)–treated *Ptpn2*$^{fl/fl}$, *Mx1*-Cre;*Ptpn2*$^{fl/fl}$, or *Mx1*-Cre;*Ptpn2*$^{fl/fl}$;*Stat5*$^{fl/+}$ mice on OP9-DL1 (Fig. 5 B) versus OP9 (Fig. 5 C) stromal cells and assessed the influence on DN2a and DN2b cell numbers and the generation of CD11c^{+} dendritic and NK1.1^{+} NK cells, respectively. *Stat5* heterozygosity corrected the increased DN2a cell numbers both in vivo (Fig. 5 A) as well as on OP9-DL1 cells ex vivo (Fig. 5 B) and the increased diversion of PTPN2-deficient DN2a cells to the NK and dendritic cell lineages when cultured on OP9 cells (Fig. 5 C). Interestingly, although DN2b cells were not significantly decreased in *Mx1*-Cre;*Ptpn2*$^{fl/fl}$ mice (Fig. 5 A), as one might expect from defective T cell lineage commitment, we noted that *Stat5* heterozygosity decreased DN2b cell numbers below those seen in *Ptpn2*$^{fl/fl}$ control mice in vivo (Fig. 5 A) or after DN2a OP9-DL1 co-culture ex vivo (Fig. 5 B). This is in keeping with the notion that enhanced STAT5 signaling promotes DN2b cell survival. To complement these studies, we also used a pharmacological approach and cultured DN2a *Ptpn2*$^{+/+}$ and *Ptpn2*$^{-/-}$ thymocytes on OP9-DL1 (Fig. 5 D) or OP9 (Fig. 5 E) stromal cells and tested whether JAK inhibition with the drug CMP6 might repress the accumulation of DN2a cells on OP9-DL1 cells (Fig. 5 D) or the generation

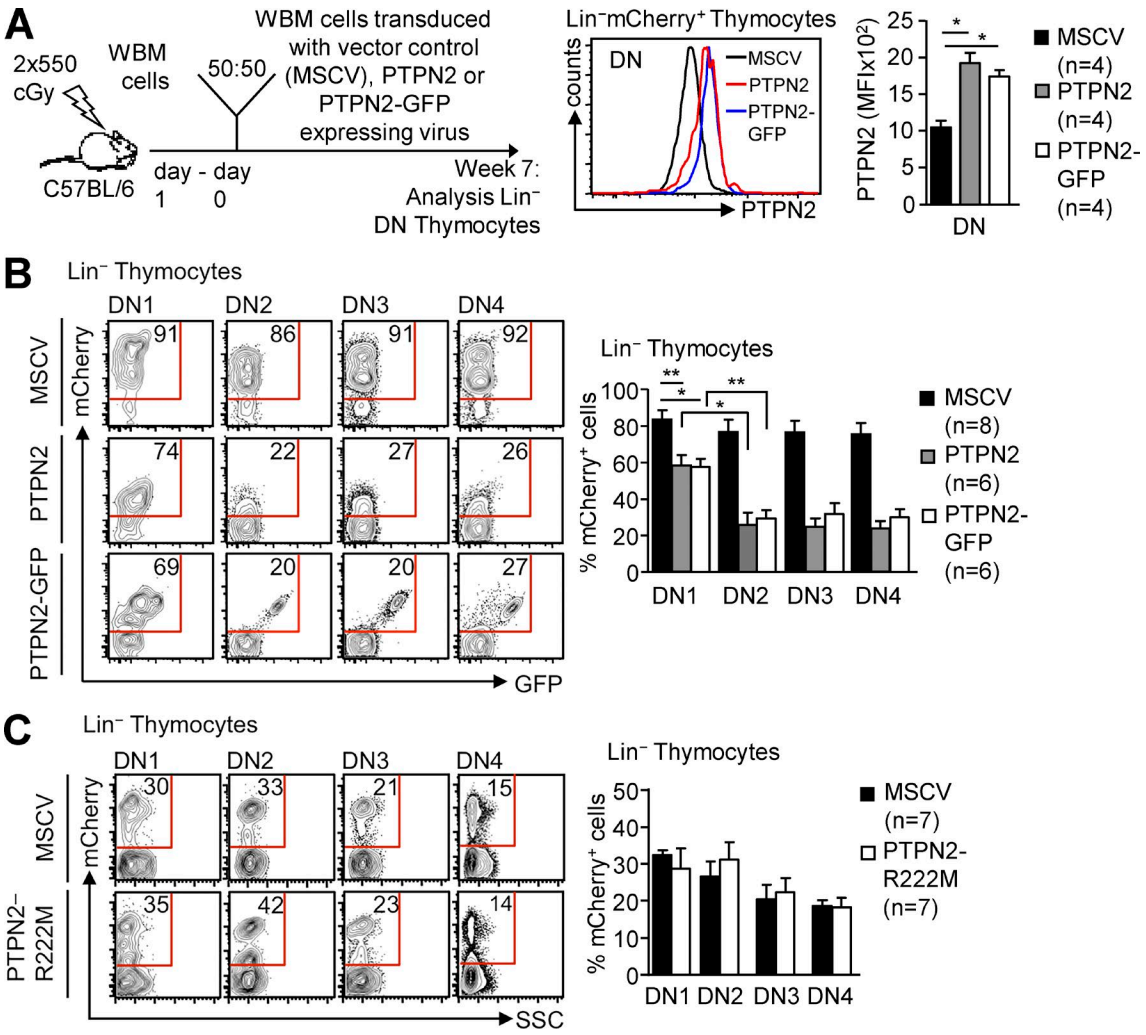

Figure 4. **PTPN2 overexpression represses DN thymocyte development.** (A–C) 5 × 10^5 WBM cells from C57BL/6 mice were transduced with control mCherry-expressing retrovirus (MSCV) or retroviruses expressing mCherry plus WT PTPN2, nuclear-restricted GFP-PTPN2 (A and B), or catalytically inactive PTPN2-R222M (C) and were transplanted into lethally irradiated (2 × 550 cGy) C57BL/6 hosts. DN thymocyte development was assessed after 7 wk. (A) Intracellular PTPN2 levels (MFI) in Lin⁻ mCherry⁺ DN thymocytes from mice reconstituted with WBM transduced with MSCV control–, WT PTPN2–, or GFP-PTPN2–expressing retroviruses were determined by flow cytometry. (B and C) Relative mCherry⁺ DN1–4 cells from mice reconstituted with WBM cells infected with control MSCV or MSCV encoding WT PTPN2 or GFP-PTPN2 (B), or mice reconstituted with WBM cells infected with control MSCV or MSCV encoding PTPN2-R222M (C). Representative results (means ± SEM; MSCV, *n* = 4–8; PTPN2, *n* = 4–6; PTPN2-GFP, *n* = 4–6; and PTPN2-R222M, *n* = 7) and representative cytometry profiles from at least two independent experiments are shown. Significance was determined using two-tailed Mann-Whitney *U* test. *, P < 0.05; **, P < 0.01.

of Lin⁻CD11c⁺ dendritic and Lin⁻NK1.1⁺ NK cells on OP9 cells (Fig. 5 E). Notably, JAK inhibition corrected the increased numbers of PTPN2-deficient DN2a cells on OP9-DL1 cells (Fig. 5 D) and the increased diversion of PTPN2-deficient DN2a cells to NK and dendritic cell lineages when cultured on OP9 cells (Fig. 5 E). In contrast, treatment with inhibitors of SFKs (SU6656 or Saracatinib [AZD0503]), which are instrumental in β selection (Molina et al., 1992; Groves et al., 1996; Palacios and Weiss, 2004), had no significant impact on DN2a cell numbers on OP9-DL1 cells (Fig. 5 D) or the generation of NK and dendritic cells on OP9 stromal cells (Fig. 5 E). These findings indicate that the increased STAT5 signaling associated with PTPN2 deficiency may contribute to the attenuation of T cell lineage commitment.

PTPN2 regulates αβ T cell development

In addition to impacting on DN2 thymocytes and T cell lineage commitment, our studies indicate that PTPN2 can also independently affect the later stages of T cell development. This is based on the observations that PTPN2 deficiency increased the numbers of DN3 and DN4 cells and the generation of DP and SP thymocytes in vivo and ex vivo, despite

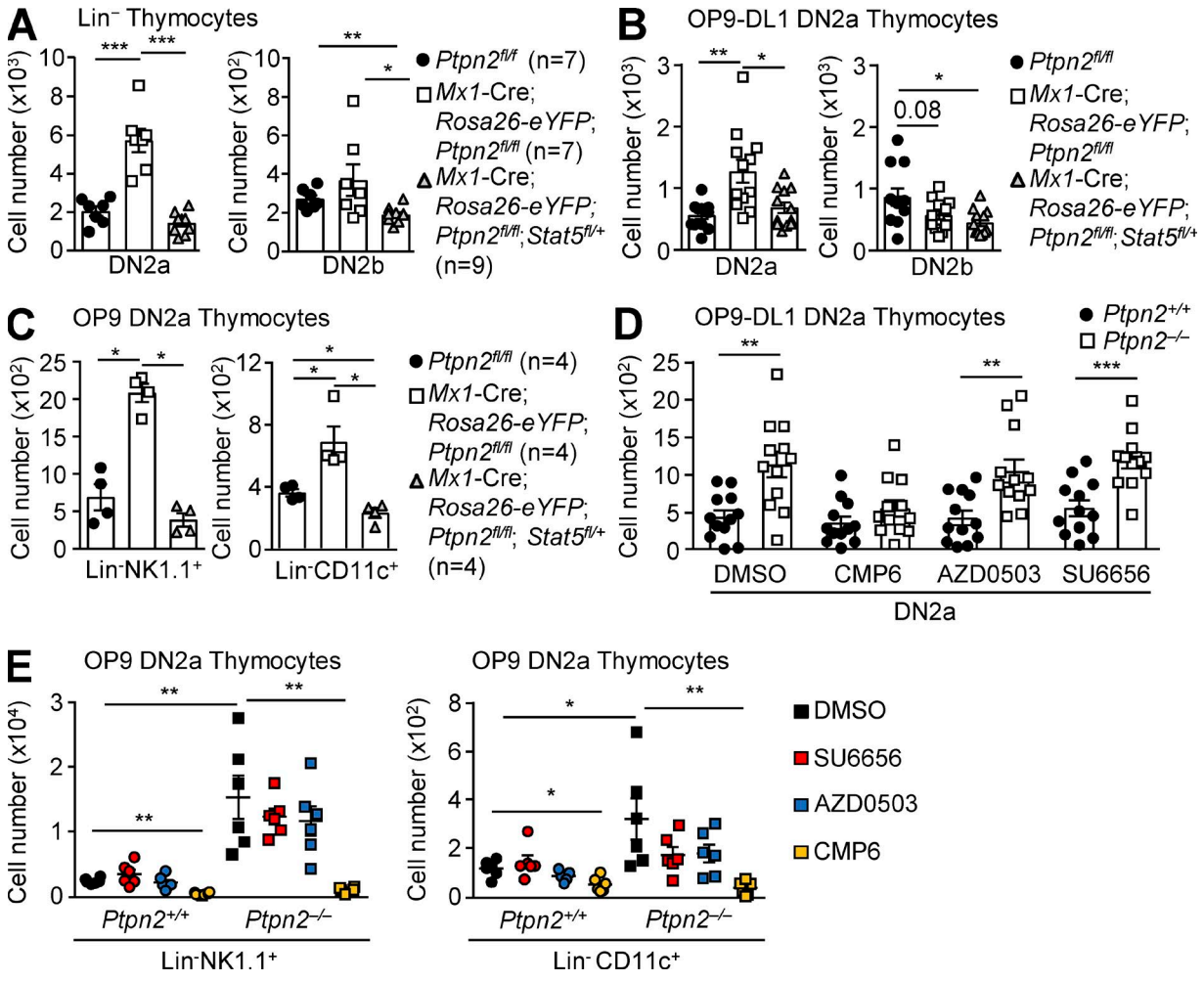

Figure 5. **PTPN2 regulates STAT5-dependent T cell lineage commitment.** (A) Lin⁻ thymocytes from poly (I:C)–treated *Rosa26-YFP;Ptpn2*$^{fl/fl}$ (C57BL/6), *Mx1*-Cre;*Rosa26-eYFP;Ptpn2*$^{fl/fl}$ (C57BL/6), and *Mx1*-Cre;*Rosa26-eYFP;Ptpn2*$^{fl/fl}$;*Stat5*$^{fl/+}$ (C57BL/6) mice were stained for CD25, CD44, and c-KIT, and DN2a and DN2b cell subsets were quantified by flow cytometry. (B and C) FACS-purified Lin⁻ DN2a thymocytes from poly (I:C)–treated *Rosa26-eYFP;Ptpn2*$^{fl/fl}$ (C57BL/6), *Mx1*-Cre;*Rosa26-eYFP;Ptpn2*$^{fl/fl}$;*Stat5*$^{+/-}$ (C57BL/6), and *Mx1*-Cre;*Rosa26-eYFP;Ptpn2*$^{fl/fl}$ (C57BL/6) mice were cultured on OP9-DL1 stromal cells for 3 d (B) or OP9 cells for 5 d (C) and then stained for c-KIT, CD44, and CD25 or lineage markers CD11c and NK1.1 and DN2a versus DN2b (B) or CD11c⁺ (C), and NK1.1⁺ cells were quantified by flow cytometry. (D and E) FACS-purified Lin⁻ DN2a thymocytes from *Ptpn2*$^{+/+}$ (C57BL/6) versus *Ptpn2*$^{-/-}$ (C57BL/6) mice were cultured on OP9-DL1 stromal cells for 3 d (D) or OP9 stromal cells for 5 d (E) in the presence of DMSO vehicle control, or the SFK PTK inhibitors SU6656 or AZD0503, or the JAK PTK inhibitor CMP6, and then stained for c-KIT, CD44, and CD25 or lineage markers CD11c and NK1.1. DN2a versus DN2b (D) or CD11c⁺ and NK1.1⁺ (E) cells were quantified by flow cytometry. Representative results (means ± SEM; *Ptpn2*$^{+/+}$, *n* = 4–6; *Ptpn2*$^{-/-}$, *n* = 4–6; *Rosa26-eYFP;Ptpn2*$^{fl/fl}$, *n* = 4–7; *Mx1*-Cre;*Rosa26-eYFP;Ptpn2*$^{fl/fl}$, *n* = 4–7; and *Mx1*-Cre;*Rosa26-eYFP;Ptpn2*$^{fl/fl}$;*STAT5*$^{fl/+}$, *n* = 4–9) from at least three (A) or two independent experiments (B–E) are shown. In B and D, triplicates from four individual mice per genotype are shown. Significance was determined using two-tailed Mann-Whitney *U* test. *, P < 0.05; **, P < 0.01; ***, P < 0.001.

DN2b cell numbers being unaltered (Figs. 1, A–C; 2, A–D; and S3, A and E–H). This suggests that PTPN2 deficiency may enhance the expansion and/or survival and differentiation of cells that transition to the DN3 stage. For successful β selection, TCR-β chains resulting from productive *Tcrb* gene rearrangement must pair with the pre–T-α protein to form the pre-TCR, which signals via the SFKs LCK and FYN to promote progression of the preselected TCR-β^{lo}CD27^{lo} DN3a cells into the post-selected TCR-β^{hi}CD27^{hi} DN3b stage (Molina et al., 1992; Groves et al., 1996; Palacios and Weiss, 2004; Taghon et al., 2006). Pre-TCR signaling promotes DN3b cell survival, proliferation, and differentiation into DN4s and thereafter into the DP stage (Palacios and Weiss, 2004). To assess the impact of PTPN2 deletion on TCR-β selection, independent of any effects on DN2 cells and T cell lineage commitment, we adopted two strategies. First, we purified c-KIT^{lo}CD27^{lo} DN3a cells by FACS and assessed their proliferation by CellTrace violet (CTV) dilution to monitor sequential cell divisions and differentiation when cultured on OP9-DL1 stromal cells (Fig. 6 A). PTPN2

deficiency did not alter the number of divisions that DN3a cells underwent when cultured on OP9-DL1 stromal cells (Fig. 6 A). This is in keeping with the unaltered Ki67 staining observed in vivo (Fig. 1 H). However, PTPN2 deficiency increased the total number of cells at each division (Fig. 6 A). This is in keeping with the increased BCL-2 and MCL-1 expression (Fig. 1 G) and increased survival of DN3 cells ex vivo (Fig. S4 C). PTPN2 deficiency also increased the differentiation of DN3a cells and the generation of TCR-β–positive cells at each cellular division (Fig. 6 A). Therefore, these results reveal that loss of PTPN2 increases DN3 survival and the generation of TCR-β cells, at least ex vivo. Next, we took advantage of *Lck*-Cre;*Ptpn2*$^{fl/fl}$ mice (Wiede et al., 2011, 2014a,b) because this *Lck*-Cre transgene (Gu et al., 1994; Hennet et al., 1995) facilitates deletion of floxed genes only after the DN2 stage (Shi and Petrie, 2012). We introduced the *RosaA26-YFP* reporter into the *Lck*-Cre;*Ptpn2*$^{fl/fl}$ strain to identify cells that had recombined their *Ptpn2*$^{fl/fl}$ alleles by YFP fluorescence. In keeping with previous studies (Hennet et al., 1995; Shi and Petrie, 2012), we found that CRE-mediated recombination of *Ptpn2*$^{fl/fl}$ was only evident after the DN2 stage, with 11 ± 1.1% of DN3 but 46 ± 3.6% of DN4 being YFP positive (Fig. S5 A). To investigate the impact of PTPN2 deletion, we compared the proportions of TCR-β^{lo}CD27^{lo} DN3a versus TCR-β^{hi}CD27^{hi} DN3b cells within the YFP-negative (i.e., PTPN2 expressing) versus YFP-positive (i.e., PTPN2 deficient) thymocyte populations (Fig. 6 B). We found that PTPN2 deficiency (marked by YFP positivity) was accompanied by an approximately threefold increase in DN3b cells and a concomitant decrease in DN3a cells (Fig. 6 B). Consistent with this, we found that the numbers of TCR-β$^+$ DN3 and DN4 cells were significantly increased in both 14-d-old *Ptpn2*$^{-/-}$ mice and in adult *Mx1*-Cre;*Ptpn2*$^{fl/fl}$ mice after poly (I:C)–induced PTPN2 deletion (Fig. 6 C). Collectively, these results demonstrate that PTPN2 deficiency enhances β selection.

PTPN2 deficiency promotes SFK-dependent β selection

At least one way by which PTPN2 may regulate β selection is through the dephosphorylation and inactivation of the proximal pre-TCR/TCR PTKs LCK and FYN (Straus and Weiss, 1992; Iwashima et al., 1994; Palacios and Weiss, 2004). The importance of these SFKs at this developmental checkpoint is demonstrated by the observations that thymocytes deficient for LCK exhibit a profound block in β selection, whereas thymocytes lacking both LCK and FYN are completely defective in progression past the DN3 stage (Molina et al., 1992; Groves et al., 1996; Palacios and Weiss, 2004). We have shown previously that LCK and FYN, but not ZAP-70, can serve as direct substrates for PTPN2 (Wiede et al., 2011) and that PTPN2 deficiency in thymocytes as well as mature T cells is accompanied by enhanced TCR/SFK signaling and T cell immune responses (Wiede et al., 2011, 2014a,b, 2017). We monitored Y394 LCK and Y416 FYN phosphorylation, markers of activation of these SFKs, using antibodies specific to Y418-phosphorylated c-SRC by flow cytometry. We found that the enhanced β selection in *Ptpn2*$^{-/-}$ mice was accompanied by increased c-SRC Y418 phosphorylation specifically at the DN3 and DN4 stages (Fig. 7 A). Enhanced SFK phosphorylation (p-SFK) and activation were also noted in DN3 and DN4 thymocytes generated in vitro by culturing WBM cells on OP9-DL1 stromal cells (Fig. 7 B). These results indicate that the enhanced β selection associated with PTPN2 deficiency is accompanied by increased SFK signaling.

To determine the extent to which the elevated SFK activation may contribute to the enhanced β selection seen in the absence of PTPN2, we first took advantage of a genetic approach. We assessed the impact of superimposing LCK deficiency on β selection (Fig. 7, C–H). We crossed *Ptpn2*$^{-/-}$ (C57BL/6) mice onto the *Lck*$^{+/-}$ (C57BL/6) heterozygous background to reduce total LCK protein by 50%. *Lck* heterozygosity had no effect on STAT5 phosphorylation in DN thymocytes (Fig. 7 C) but reduced the otherwise increased p-SFK in *Ptpn2*$^{-/-}$ DN3, DN4, DP, and SP thymocytes so that p-SFK more closely approximated that found in *Ptpn2*$^{+/+}$ controls (Fig. 7, D and E). These results demonstrate that PTPN2 primarily affects LCK Y394 phosphorylation in thymocytes. *Lck* heterozygosity had no impact on DN1 or DN2 cell numbers but completely corrected the increase in DN3, DN4, and TCR-β$^+$ thymocytes otherwise associated with PTPN2 deficiency (Fig. 7 F). Moreover, *Lck* heterozygosity corrected the increases in DP and SP thymocytes and peripheral splenic CD4$^+$, as well as CD8$^+$ T cells otherwise associated with PTPN2 deficiency at 14 d of age (Fig. 7 G). To determine whether the effects on β selection were cell intrinsic, we cultured purified DN3a thymocytes from *Ptpn2*$^{+/+}$, *Ptpn2*$^{-/-}$, or *Ptpn2*$^{-/-}$;*Lck*$^{+/-}$ mice on OP9-DL1 stromal cells in the presence of FLT3L and IL-7 and assessed the generation of TCR-β$^+$ thymocytes after 4 d (Fig. 7 H). *Lck* heterozygosity corrected the enhanced generation of TCR-β$^+$ thymocytes (Fig. 7 H). In contrast, *Stat5* heterozygosity in PTPN2-deficient DN3a thymocytes (i.e., isolated from poly (I:C)–treated *Mx1*-Cre;*Ptpn2*$^{fl/fl}$;*Stat5*$^{fl/+}$ mice) did not correct the enhanced generation of TCR-β$^+$ thymocytes evident when DN3a thymocytes from poly (I:C)–treated *Mx1*-Cre;*Ptpn2*$^{fl/fl}$ mice where cultured on OP9-DL1 cells (Fig. 7 I). These results indicate that PTPN2 deficiency drives β selection and T cell development specifically through the promotion of LCK, but not STAT5, signaling.

To complement our genetic studies and to further explore the cell-intrinsic contributions of SFK signaling in the promotion of β selection, we also treated PTPN2-deficient YFP$^+$ DN3a thymocytes (from *Lck*-Cre;*Ptpn2*$^{fl/fl}$;*RosaA26-YFP* mice) differentiating in vitro with SU6656 or Saracatinib (AZD0503) and assessed the impact of these SFK inhibitors on the generation of DN3 and DN4 cells and the total numbers of T lymphoid cells. Both drugs repressed the enhanced SFK signaling in PTPN2-deficient DN3 and DN4 cells to the levels seen in YFP$^-$ control thymocytes (Fig. 8 A), and this significantly diminished the increase in the num-

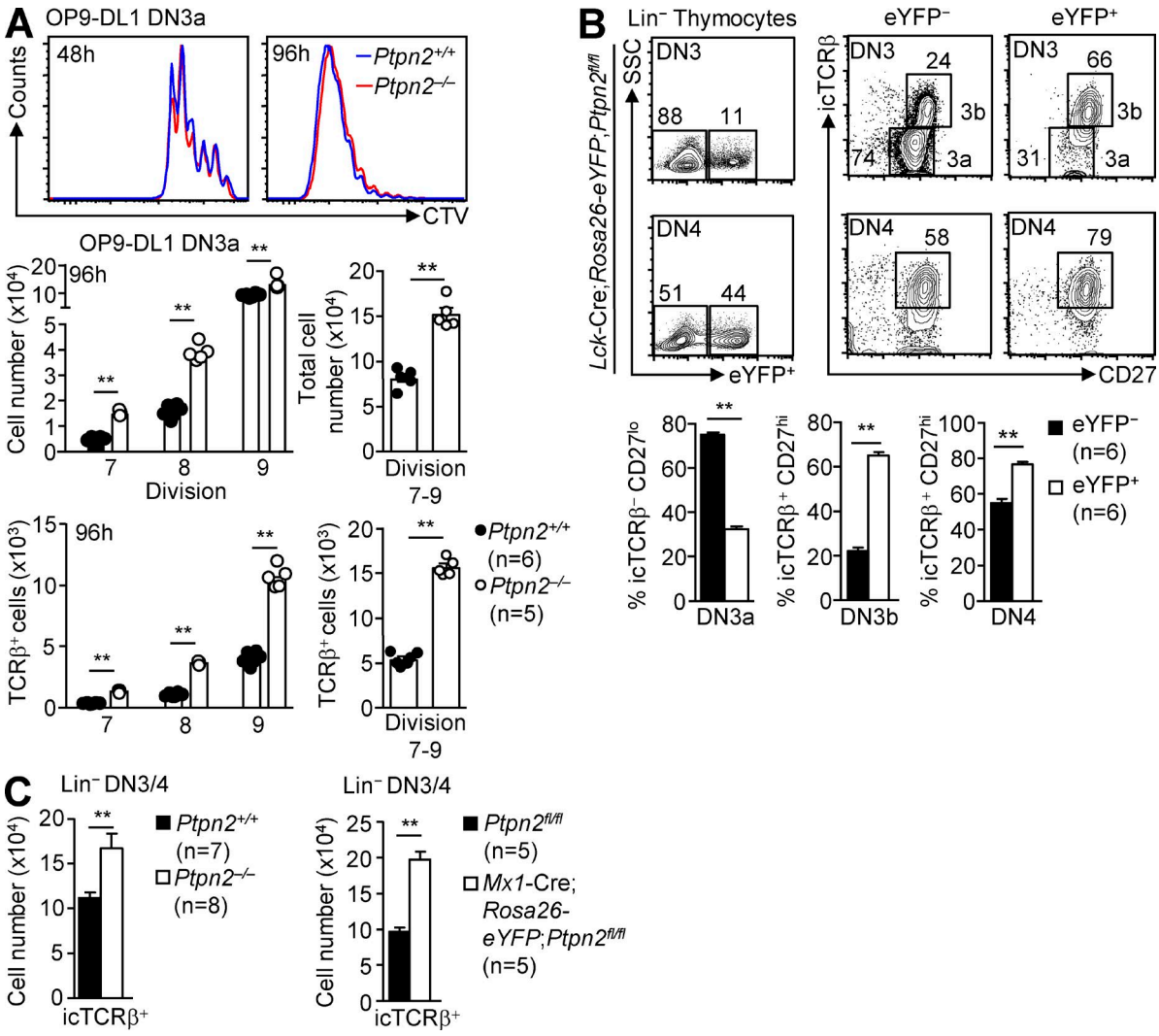

Figure 6. **PTPN2 deficiency enhances β selection.** (A) FACS-purified, CTV-labeled Lin⁻ DN3a thymocytes from *Ptpn2*$^{+/+}$ (C57BL/6) and *Ptpn2*$^{-/-}$ (C57BL/6) mice were cultured on OP9-DL1 stromal cells. Thymocytes were harvested after 48 or 96 h and stained for TCR-β and CD45 and then examined by flow cytometry for CTV dilution. *Ptpn2*$^{-/-}$ (C57BL/6) versus *Ptpn2*$^{+/+}$ (C57BL/6) total CD45$^+$ thymocytes or CD45$^+$TCR-β^{hi} cells per division and the generation of total CD45$^+$ thymocytes or CD45$^+$TCR-β^{hi} cells were determined. (B) Lin$^-$ thymocytes from *Lck*-Cre;*Rosa26-YFP;Ptpn2*$^{fl/fl}$ (C57BL/6) mice were stained for CD25, CD44, CD27, and intracellular TCR-β. DN3 (CD25$^+$CD44$^-$) and DN4 (CD25$^-$CD44$^-$) thymocytes were gated for eYFP$^-$ (PTPN2 expressing) and eYFP$^+$ (PTPN2 deleted) cells, and the relative DN3a (intracellular TCR-β^{hi}CD27^{lo}), DN3b (intracellular TCR-β^{hi}CD27^{hi}), and DN4 (intracellular TCR-β^{hi}CD27^{hi}) cell abundance was determined by flow cytometry. (C) Lin$^-$ thymocytes from *Ptpn2*$^{+/+}$ (C57BL/6) and *Ptpn2*$^{-/-}$ (C57BL/6) mice or poly (I:C)–treated *Rosa26-eYFP;Ptpn2*$^{fl/fl}$ (C57BL/6) and *Mx1*-Cre;*Rosa26-eYFP;Ptpn2*$^{fl/fl}$ (C57BL/6) mice were stained for CD25, CD44, and intracellular TCR-β (icTCRβ$^+$). icTCRβ$^+$ DN3 (CD25$^+$CD44$^-$) and (CD25$^-$CD44$^-$) DN4 cell numbers were quantified by flow cytometry. Representative results (means ± SEM; *Ptpn2*$^{+/+}$, *n* = 6–7; *Ptpn2*$^{-/-}$, *n* = 5–8; *Lck*-Cre;*Rosa26-YFP;Ptpn2*$^{fl/fl}$, *n* = 6; *Rosa26-eYFP;Ptpn2*$^{fl/fl}$, *n* = 5; and *Mx1*-Cre;*Rosa26-eYFP;Ptpn2*$^{fl/fl}$, *n* = 5) (A–C) and representative cytometry profiles (A and B) from at least three independent experiments are shown. Significance was determined using two-tailed Mann-Whitney *U* test. **, P < 0.01.

bers of DN3/DN4 cells (Fig. 8 B) and the overall numbers of thymocytes (Fig. S5 B). Finally, we assessed the relative contributions of the SFK versus JAK/STAT5 signaling pathways to the enhanced β selection and increased generation of TCR-β$^+$ thymocytes associated with PTPN2 deficiency by incubating PTPN2-deficient YFP$^+$ DN3a thymocytes differentiating ex vivo with the SFK inhibitor SU6656 or the JAK inhibitor CMP6. SU6656 corrected the increased generation of TCR-β$^+$ thymocytes, whereas CMP6 had no significant impact (Fig. 8 C). Collectively, these genetic and pharmacological inhibitor studies demonstrate that PTPN2 controls β selection through the specific dephosphorylation and inactivation of the SFK LCK.

PTPN2 deficiency promotes SFK- and STAT5-dependent γδ TCR T cell development

The development of DN3 cells into αβ TCR versus γδ TCR T cells is thought to be dependent on TCR signal strength,

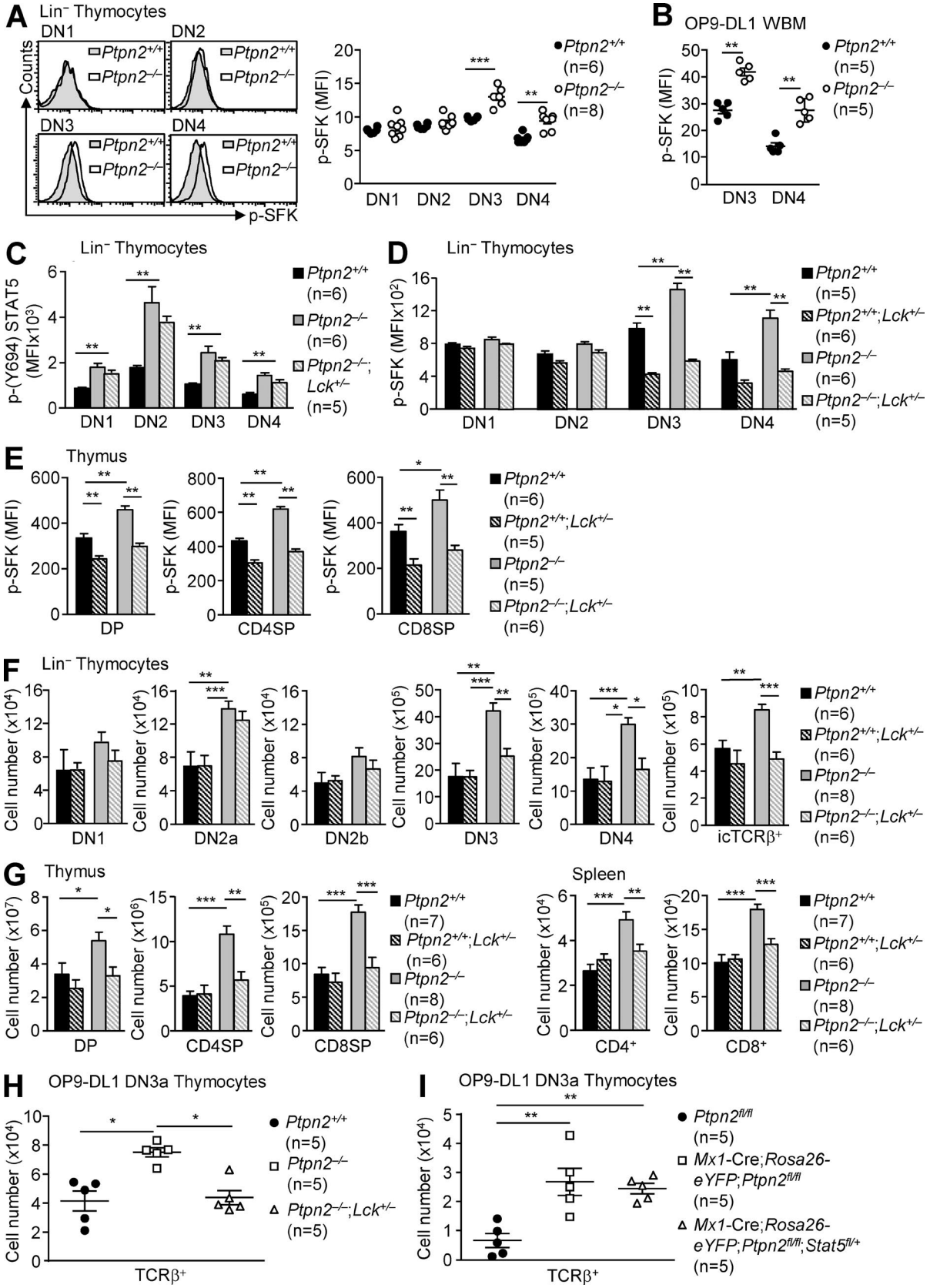
A
Lin⁻ Thymocytes
DN1
DN2
DN3
DN4
Counts
Ptpn2+/+
Ptpn2–/–
p-SFK
p-SFK (MFI)
DN1 DN2 DN3 DN4
Ptpn2+/+ (n=6)
Ptpn2–/– (n=8)
B
OP9-DL1 WBM
p-SFK (MFI)
DN3 DN4
Ptpn2+/+ (n=5)
Ptpn2–/– (n=5)
C
Lin⁻ Thymocytes
p-(Y694) STAT5 (MFIx10³)
DN1 DN2 DN3 DN4
Ptpn2+/+ (n=6)
Ptpn2–/– (n=6)
Ptpn2–/–;Lck+/– (n=5)
D
Lin⁻ Thymocytes
p-SFK (MFIx10²)
DN1 DN2 DN3 DN4
Ptpn2+/+ (n=5)
Ptpn2+/+;Lck+/– (n=6)
Ptpn2–/– (n=6)
Ptpn2–/–;Lck+/– (n=5)
E
Thymus
p-SFK (MFI)
DP
CD4SP
CD8SP
Ptpn2+/+ (n=6)
Ptpn2+/+;Lck+/– (n=5)
Ptpn2–/– (n=5)
Ptpn2–/–;Lck+/– (n=6)
F
Lin⁻ Thymocytes
Cell number (x10⁴)
Cell number (x10⁵)
DN1
DN2a
DN2b
DN3
DN4
icTCRβ+
Ptpn2+/+ (n=6)
Ptpn2+/+;Lck+/– (n=6)
Ptpn2–/– (n=8)
Ptpn2–/–;Lck+/– (n=6)
G
Thymus
Spleen
Cell number (x10⁷)
Cell number (x10⁶)
Cell number (x10⁵)
Cell number (x10⁴)
DP
CD4SP
CD8SP
CD4⁺
CD8⁺
Ptpn2+/+ (n=7)
Ptpn2+/+;Lck+/– (n=6)
Ptpn2–/– (n=8)
Ptpn2–/–;Lck+/– (n=6)
H
OP9-DL1 DN3a Thymocytes
Cell number (x10⁴)
TCRβ+
Ptpn2+/+ (n=5)
Ptpn2–/– (n=5)
Ptpn2–/–;Lck+/– (n=5)
I
OP9-DL1 DN3a Thymocytes
Cell number (x10⁴)
TCRβ+
Ptpn2fl/fl (n=5)
Mx1-Cre;Rosa26-eYFP;Ptpn2fl/fl (n=5)
Mx1-Cre;Rosa26-eYFP;Ptpn2fl/fl;Stat5fl/+ (n=5)

with strong TCR signaling favoring γδ TCR T cell development and weaker signaling favoring αβ TCR T cell development (Haks et al., 2005; Hayes et al., 2005; Kreslavsky et al., 2008; Fahl et al., 2014; Zarin et al., 2015; Muñoz-Ruiz et al., 2016). TCR signal strength further variably influences the generation of IL-17 (IL-17$^+$)– versus IFN-γ (IFN-γ$^+$)–producing γδ T cell subsets (Jensen et al., 2008; Ribot et al., 2009; Turchinovich and Hayday, 2011; Prinz et al., 2013; Muñoz-Ruiz et al., 2016). Both TCR-γδ and pre-TCR signaling are reliant on SFKs, as reflected by the complete absence of both αβ TCR and γδ TCR T cells and the accumulation of DN3 thymocytes in *Lck*$^{-/-}$*Fyn*$^{-/-}$ mice (Molina et al., 1992; Groves et al., 1996). Beyond TCR signal strength, other factors can also contribute to the thymic generation of γδ TCR T cells. They include IL-7, which signals through STAT5 to influence TCR-γ gene rearrangement and expression (Kang et al., 1999, 2001; Ye et al., 2001). Given that PTPN2 deficiency enhanced both SFK and STAT5 signaling, we reasoned that the absence of PTPN2 might also drive the generation of γδ TCR T cells. Indeed, we found that γδ TCR thymocytes were increased by 2.7-fold in *Ptpn2*$^{-/-}$ mice (Fig. 9 A) and by 4.5-fold in adult *Mx1*-Cre;*Ptpn2*$^{fl/fl}$ mice after PTPN2 deletion (Fig. 9 B). In particular, we found that PTPN2 deficiency increased the development of IFN-γ$^+$ TCR-δ$^+$ thymocytes (Fig. 9 C). In contrast, the development of CD1d-dependent TCR-β$^+$ NKT cells, which arise from DP thymocytes expressing randomly generated semi-invariant lipid-binding TCRs (Godfrey et al., 2010), was unaltered (Fig. 9 D), whereas the generation of CD4$^+$CD25$^+$FoxP3$^+$ regulatory T cells (T reg cells) was increased (Fig. 9 D). The latter is in agreement with a study demonstrating that the PTPN2-mediated inhibition of IL-2–induced JAK/STAT5 signaling represses the thymic generation of T reg cells (Yi et al., 2014). To determine whether PTPN2 deficiency may promote the cell-autonomous differentiation of γδ TCR thymocytes, we cultured CTV-stained, FACS-purified c-KIT^{lo}CD27^{lo} DN3a cells on OP9-DL1 stromal cells and assessed the generation of TCR-δ$^+$ thymocytes at each cellular division. PTPN2 deficiency did not alter the proliferation of DN3 cells, as assessed by the dilution of CTV dye (not depicted), but resulted in increased TCR-δ$^+$ thymocyte development at each cellular division (Fig. 9 E). This is consistent with the increased generation of γδ TCR thymocytes being an outcome of enhanced differentiation. Importantly, the increase in γδ TCR thymocytes was associated with a 9.5-fold increase in intestinal TCR-δ$^+$ CD3$^+$ intraepithelial lymphocytes (IELs) and a 5.5-fold increase in lamina propria (LP) TCR-δ$^+$ CD3$^+$ T cells in adult *Mx1*-Cre;*Ptpn2*$^{fl/fl}$ mice 4 wk after PTPN2 deletion (Fig. 9 F). Most of the TCR-δ$^+$ CD3$^+$ T cells were IFN-γ$^+$ γδ TCR T cells (Fig. 9 G). Collectively, these results demonstrate that PTPN2 deficiency enhances γδ TCR T cell development.

To determine whether PTPN2 deficiency may drive γδ TCR T cell development through the enhancement of SFK and/or STAT5 signaling, we assessed the generation of TCR-δ$^+$ cells in PTPN2-deficient thymocytes heterozygous for *Lck* or *Stat5*. *Lck* heterozygosity partially decreased the elevated TCR-δ$^+$ thymocyte generation in *Ptpn2*$^{-/-}$ mice (Fig. 9 H). *Lck* heterozygosity also tended to decrease TCR-δ$^+$ thymocyte generation ex vivo when PTPN2-deficient DN3a thymocytes were co-cultured with OP9-DL1 stromal cells (Fig. 9 I). Conversely, *Stat5* heterozygosity completely reversed the increased TCR-δ$^+$ thymocyte generation ex vivo (Fig. 9 J) but had no effect on TCR-β$^+$ thymocyte generation (Fig. 7 I). To complement these studies, we also assessed the impact of SFK versus JAK inhibition on the generation of TCR-δ$^+$ thymocytes when DN3a cells were cultured on OP9-DL1 cells. The inhibition of SFKs with SU6656 partially decreased the enhanced generation of *Ptpn2*$^{-/-}$ TCR-δ$^+$ thymocytes (Fig. 9 K), whereas JAK inhibition with CMP6 completely reversed the increased TCR-δ$^+$ thymocyte generation (Fig. 9 K). Collectively, these results indicate that the enhanced STAT5 signaling associated with PTPN2 deficiency is essential for the increased differentiation of DN3 cells to

Figure 7. **PTPN2 deficiency promotes LCK-dependent β selection.** (A) Lin$^-$ thymocytes from *Ptpn2*$^{+/+}$ (C57BL/6) and *Ptpn2*$^{-/-}$ (C57BL/6) mice were stained for cell surface CD25, CD44, or intracellular SFK phosphorylation (p-SFK) with antibodies to Y418-phosphorylated c-SRC, and DN1–4 p-SFK MFIs were determined by flow cytometry. (B) WBM cells from *Ptpn2*$^{+/+}$ (C57BL/6) and *Ptpn2*$^{-/-}$ (C57BL/6) mice were cultured for 9 d on OP9-DL1 stromal cells. DN3–4 p-SFK MFIs were determined by flow cytometry. (C) Lin$^-$ thymocytes from *Ptpn2*$^{+/+}$ (C57BL/6), *Ptpn2*$^{-/-}$ (C57BL/6), and *Ptpn2*$^{-/-}$;*Lck*$^{+/-}$ (C57BL/6) mice were stained for CD25, CD44, and intracellular p-STAT5, and DN1–4 p-STAT5 MFIs were determined by flow cytometry. (D and E) Lin$^-$ thymocytes (D) or total thymocytes (E) from *Ptpn2*$^{+/+}$(C57BL/6), *Ptpn2*$^{+/+}$;*Lck*$^{+/-}$ (C57BL/6), *Ptpn2*$^{-/-}$ (C57BL/6), or *Ptpn2*$^{-/-}$;*Lck*$^{+/-}$ (C57BL/6) mice were stained for CD25 and CD44 (D) or CD4 and CD8 (E), and DN1–4 p-SFK MFIs (D) or DP and SP p-SFK MFIs (E) were determined by flow cytometry. (F) Lin$^-$ thymocytes from *Ptpn2*$^{+/+}$(C57BL/6), *Ptpn2*$^{+/+}$;*Lck*$^{+/-}$ (C57BL/6), *Ptpn2*$^{-/-}$ (C57BL/6), and *Ptpn2*$^{-/-}$;*Lck*$^{+/-}$ (C57BL/6) mice were stained for CD25, CD44, c-KIT, and intracellular TCR-β (icTCRβ$^+$) and DN cell subsets, and icTCRβ$^+$ cells were quantified by flow cytometry. (G) Thymocytes or splenocytes from *Ptpn2*$^{+/+}$ (C57BL/6), *Ptpn2*$^{+/+}$;*Lck*$^{+/-}$ (C57BL/6), *Ptpn2*$^{-/-}$ (C57BL/6), and *Ptpn2*$^{-/-}$;*Lck*$^{+/-}$ (C57BL/6) mice were stained for CD4, CD8, and DP. CD4 SP and CD8 SP thymocytes or CD4$^+$ and CD8$^+$ T cells were quantified by flow cytometry. (H and I) FACS-purified Lin$^-$ DN3a thymocytes from *Ptpn2*$^{+/+}$ (C57BL/6), *Ptpn2*$^{-/-}$ (C57BL/6), or *Ptpn2*$^{-/-}$;*Lck*$^{+/-}$ (C57BL/6) mice (H) or from poly (I:C)–treated *Rosa26-YFP*;*Ptpn2*$^{fl/fl}$ (C57BL/6), *Mx1*-Cre;*Rosa26-eYFP*;*Ptpn2*$^{fl/fl}$ (C57BL/6), and *Mx1*-Cre;*Rosa26-eYFP*;*Ptpn2*$^{fl/fl}$;*Stat5*$^{fl/+}$ (C57BL/6) mice (I) were cultured on OP9-DL1 stromal cells for 4 d. Cells were harvested and stained for TCR-β. TCR-β$^+$ T cell numbers were determined by flow cytometry. Representative results (means ± SEM; *Ptpn2*$^{+/+}$, *n* = 5–7; *Ptpn2*$^{-/-}$, *n* = 5–8; *Ptpn2*$^{+/+}$;*Lck*$^{+/-}$, *n* = 5–6; *Ptpn2*$^{-/-}$;*Lck*$^{+/-}$, *n* = 5–6; *Rosa26-eYFP*;*Ptpn2*$^{fl/fl}$, *n* = 5; *Mx1*-Cre;*Rosa26-eYFP*;*Ptpn2*$^{fl/fl}$, *n* = 5; and *Mx1*-Cre;*Rosa26-eYFP*;*Ptpn2*$^{fl/fl}$;*STAT5*$^{fl/+}$, *n* = 5) and representative cytometry profiles (A) from at least two (C–I) or three (A and B) independent experiments are shown. Significance was determined using two-tailed Mann-Whitney *U* test. *, P < 0.05; **, P < 0.01; ***, P < 0.001.

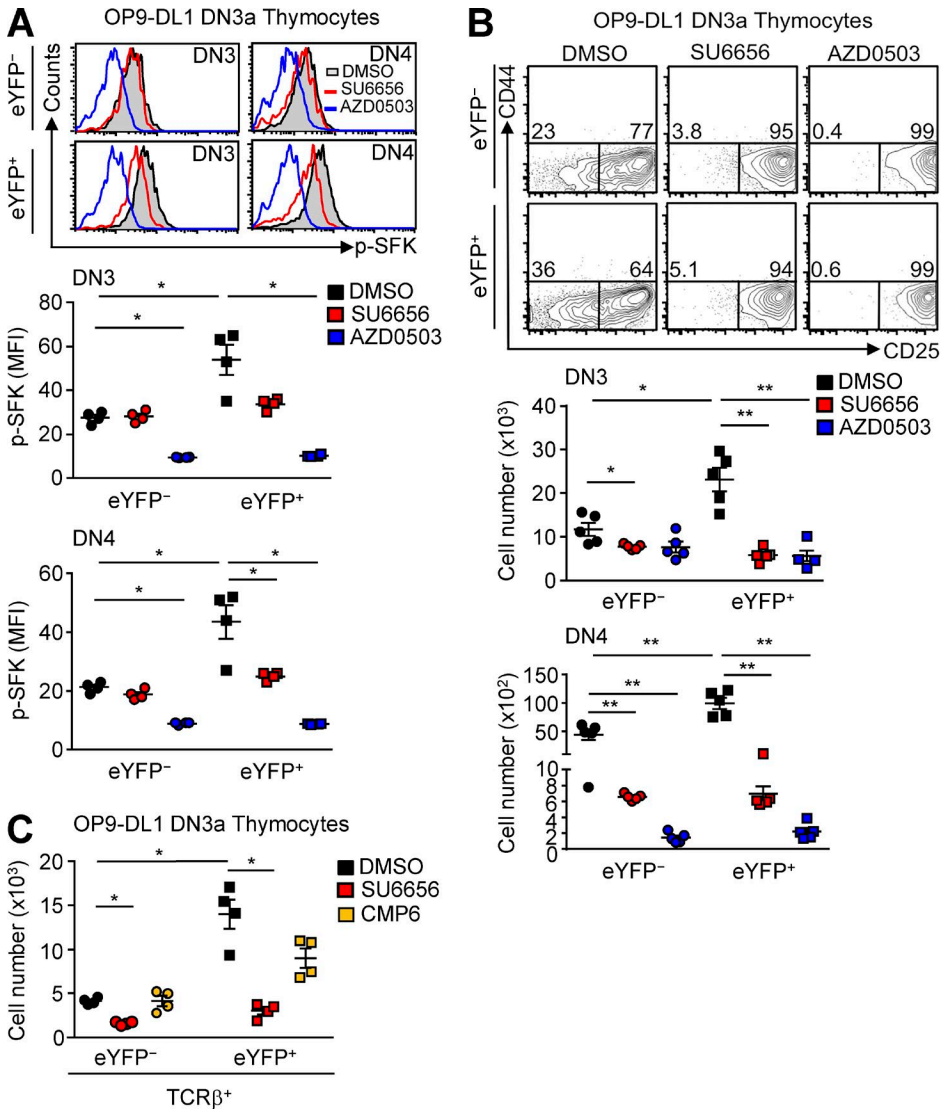

Figure 8. **SFK inhibition corrects the enhanced β selection associated with PTPN2 deficiency.** (A–C) DN3a eYFP⁻ (i.e., PTPN2 expressing) cells from *Rosa26-YFP;Ptpn2*$^{fl/fl}$ (C57BL/6) mice or DN3a eYFP⁺ (i.e., PTPN2 deleted) cells from *Lck*-Cre;*Rosa26-YFP;Ptpn2*$^{fl/fl}$ (C57BL/6) mice were cultured on OP9-DL1 stromal cells in the presence of DMSO vehicle control, or the SFK PTK inhibitors SU6656 or AZD0503 (A and B), and SU6656 or the PTK JAK inhibitor CMP6 (C). (A) p-SFK MFIs in DN3 and DN4 thymocytes were determined by flow cytometry. (B) DN3 and DN4 cell numbers were determined by flow cytometry. (C) TCR-β⁺ T cell numbers were determined by flow cytometry. Representative results (means ± SEM; *Rosa26-YFP;Ptpn2*$^{fl/fl}$, $n = 4$; and *Lck*-Cre;*Rosa26-YFP;Ptpn2*$^{fl/fl}$, $n = 4$) and representative cytometry profiles from at least two (C) or three (A and B) independent experiments are shown. Significance was determined using two-tailed Mann-Whitney *U* test. *, $P < 0.05$; **, $P < 0.01$.

the γδ TCR T cell lineage. Therefore, both elevated STAT5 and TCR/LCK signaling may contribute to the increased generation of γδ TCR T cells in PTPN2-deficient mice. This contrasts with the dependence on elevated SFK/LCK, but not STAT5 signaling, for the increased β selection and αβ TCR T cell generation accompanying PTPN2 deficiency.

PTPN2 is elevated in DN2/3 cells postnatally to repress γδ TCR T cell development

γδ TCR T cells first appear during fetal thymic ontogeny before αβ TCR T cell maturation. In adults, the proportion of γδ TCR T cells declines so that they constitute only 1–4% of the total TCR$^+$ T cells in the thymus and peripheral lymphoid organs (Prinz et al., 2013; Chien et al., 2014). The molecular basis for the postnatal decline in γδ TCR T cell production remains unclear. We investigated whether PTPN2 levels may be increased postnatally to suppress TCR-induced SFK and STAT5 signaling and thereby diminish the development of γδ TCR T cells. The proportion of thymic TCR-δ$^+$ cells was lower in 6-wk-old adult mice compared with embryonic day 18 (E18) embryos, and this was accompanied by a significant increase in TCR-β$^+$ thymocytes (Fig. 10 A). Im-

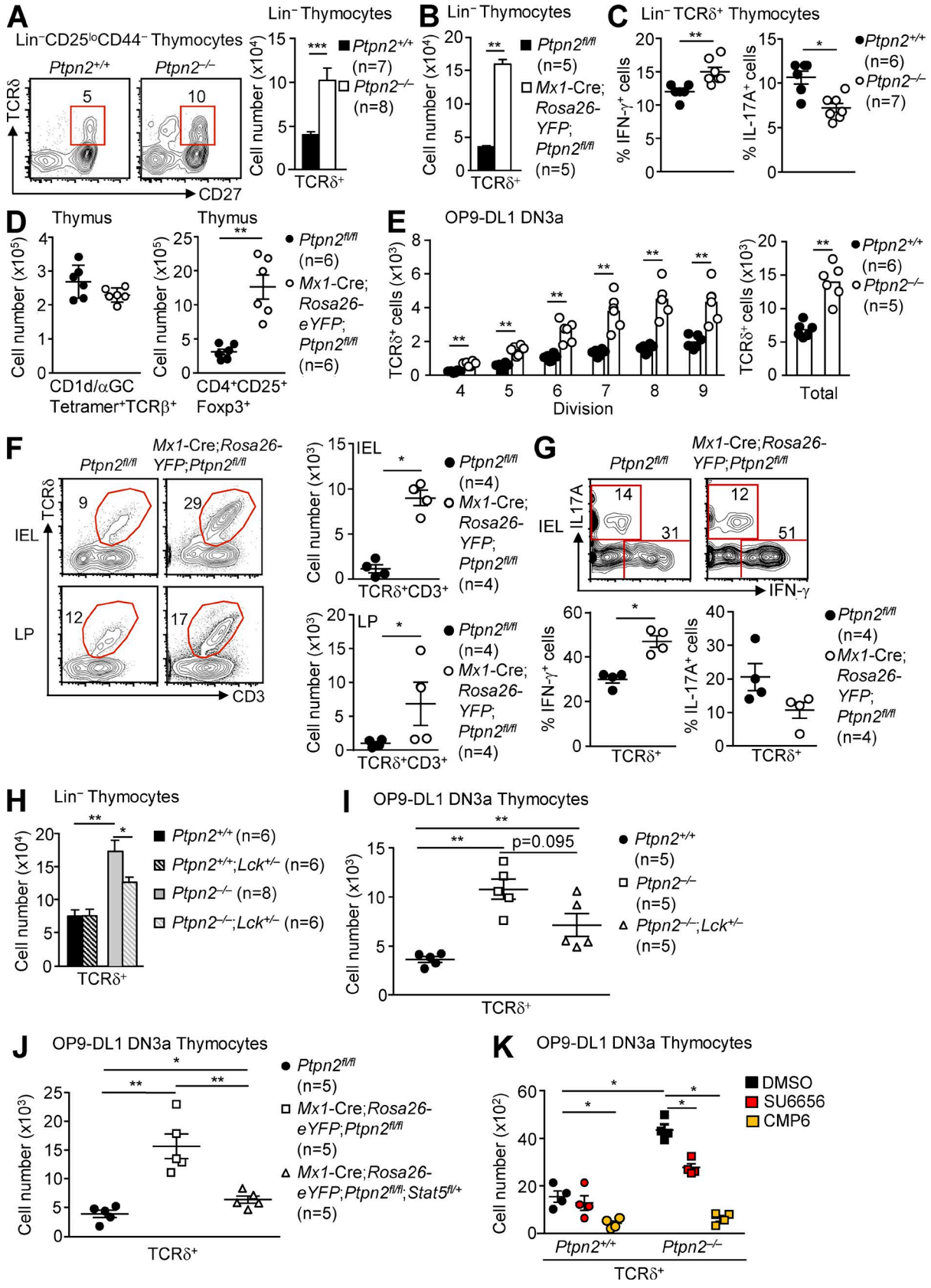
A
Lin⁻CD25^loCD44⁻ Thymocytes
Ptpn2+/+
Ptpn2−/−
TCRδ
CD27
5
10
Lin⁻ Thymocytes
Cell number (x10⁴)
TCRδ+
Ptpn2+/+ (n=7)
Ptpn2−/− (n=8)
B
Lin⁻ Thymocytes
Ptpn2fl/fl (n=5)
Mx1-Cre; Rosa26-YFP; Ptpn2fl/fl (n=5)
C
Lin⁻ TCRδ+ Thymocytes
% IFN-γ+ cells
% IL-17A+ cells
Ptpn2+/+ (n=6)
Ptpn2−/− (n=7)
D
Thymus
Cell number (x10⁵)
CD1d/αGC Tetramer+TCRβ+
CD4+CD25+ Foxp3+
Ptpn2fl/fl (n=6)
Mx1-Cre; Rosa26-eYFP; Ptpn2fl/fl (n=6)
E
OP9-DL1 DN3a
TCRδ+ cells (x10³)
Division
Total
Ptpn2+/+ (n=6)
Ptpn2−/− (n=5)
F
Ptpn2fl/fl
Mx1-Cre;Rosa26-YFP;Ptpn2fl/fl
IEL
LP
TCRδ
CD3
9
29
12
17
Cell number (x10³)
TCRδ+CD3+
Ptpn2fl/fl (n=4)
Mx1-Cre; Rosa26-YFP; Ptpn2fl/fl (n=4)
G
IL17A
IFN-γ
14
31
12
51
% IFN-γ+ cells
% IL-17A+ cells
TCRδ+
H
Lin⁻ Thymocytes
Ptpn2+/+ (n=6)
Ptpn2+/+;Lck+/− (n=6)
Ptpn2−/− (n=8)
Ptpn2−/−;Lck+/− (n=6)
I
OP9-DL1 DN3a Thymocytes
p=0.095
Ptpn2+/+ (n=5)
Ptpn2−/− (n=5)
Ptpn2−/−;Lck+/− (n=5)
J
OP9-DL1 DN3a Thymocytes
Ptpn2fl/fl (n=5)
Mx1-Cre;Rosa26-eYFP;Ptpn2fl/fl (n=5)
Mx1-Cre;Rosa26-eYFP;Ptpn2fl/fl;Stat5fl/+ (n=5)
K
OP9-DL1 DN3a Thymocytes
Cell number (x10²)
DMSO
SU6656
CMP6
Ptpn2+/+
Ptpn2−/−

portantly, we found that PTPN2 levels (as assessed by flow cytometry using a validated PTPN2 antibody; Wiede et al., 2014a) in 6-wk-old mice were increased by approximately twofold in DN2 and DN3 cells when compared with the DN1 cells but then declined at the DN4 stage (Fig. 10 B). In contrast, the increase in PTPN2 in DN2/DN3 versus DN1 cells was modest in E18 (Fig. 10 B) or E16 embryos (Fig. S5 C). These results are consistent with the notion that PTPN2 is a critical regulator of the DN2 and DN3 developmental checkpoints. Moreover, these results suggest that the relative increase in PTPN2 might suppress SFK and STAT5 signaling in adult versus embryonic DN2/3 thymocytes and repress the postnatal development of γδ TCR T cells. To explore this, we compared the impact of PTPN2 deficiency on TCR-β^+ versus TCR-δ^+ thymocyte development in E18 embryos versus 16-d-old mice. PTPN2 deficiency increased the total numbers of TCR-β^+ and TCR-δ^+ thymocytes in E18 embryos (Fig. 10 C). However, whereas relative TCR-δ^+ thymocyte abundance declined in 16-d-old versus E18 *Ptpn2*$^{+/+}$ control mice, the proportion of TCR-δ^+ thymocytes in 16-d-old *Ptpn2*$^{-/-}$ mice remained elevated and was comparable to that of E18 *Ptpn2*$^{-/-}$ embryos, so that the relative abundance of TCR-β^+ thymocytes declined and the TCR-δ/TCR-β ratio increased (Fig. 10, D–F). These findings are consistent with the notion that the postnatal increase in PTPN2 at the DN2/3 stages may contribute to the postnatal reduction in γδ TCR T cell production.

DISCUSSION

We have taken advantage of different mouse models and genetic and pharmacological approaches to establish that PTPN2 deficiency promotes STAT5-dependent DN2a cellular expansion and survival and represses T cell lineage commitment in a cell-autonomous manner. The repression of STAT5 signaling is required for the optimal induction of *Bcl11b* expression and the irreversible commitment of otherwise multipotent progenitors to the T cell lineage (Ikawa et al., 2010; Kueh et al., 2016). Although previous studies have suggested that this may be caused by a reduction in the cell surface levels of IL-7R-α (Yu et al., 2004; Ikawa et al., 2010), we found that IL-7R-α levels were not significantly reduced at the DN2b stage and instead that the repression of STAT5 signaling, induction of *Bcl11b*, and differentiation of DN2a cells to the DN2b stage may be mediated by an increase in PTPN2. In the absence of PTPN2, STAT5 Y694 phosphorylation (a marker of STAT5 activation) was markedly increased and accompanied by increased DN2a cells in the absence of any commensurate increase in DN2b cells. Conversely, the increase in *Bcl11b* that normally occurs as cells transition into DN2b was decreased and, importantly, was accompanied by the increased generation of non–T lymphoid lineage cells. Inhibitors of the JAK/STAT5 pathway, but not inhibitors of SFKs, not only attenuated the expansion of DN2a cells ex vivo but also inhibited the generation of NK and dendritic cells that otherwise resulted from the co-culture of PTPN2-deficient DN2a cells with OP9 stromal cells with or without Notch ligand. Collectively, these results are consistent with PTPN2 deficiency repressing the DN2a to DN2b transition, thus impairing T cell lineage commitment. A caveat is that PTPN2 deficiency and the enhancement of STAT5 signaling did not lead to a reduction of DN2b cells. One reason for this might be that STAT5 can also regulate the survival of DN2b cells, so that the enhanced DN STAT5 signaling associated with PTPN2 deficiency may not only repress the progression to the DN2b stage, but also promote the survival of cells that ultimately transition to this stage. Consistent with this, we found that expression of the prosurvival proteins BCL-2 and MCL-1 in DN2b cells

Figure 9. **PTPN2 deficiency promotes STAT5- and LCK-dependent γδ TCR T cell development.** (A and B) Lin$^-$ thymocytes from *Ptpn2*$^{+/+}$ (C57BL/6) and *Ptpn2*$^{-/-}$ (C57BL/6) mice (A) or from poly (I:C)–treated *Rosa26-eYFP;Ptpn2*$^{fl/fl}$ (C57BL/6) and *Mx1*-Cre;*Rosa26-eYFP;Ptpn2*$^{fl/fl}$ (C57BL/6) mice (B) were stained for CD25, CD44, CD27, and TCR-δ. The numbers of TCR-γδ$^+$ thymocytes were quantified by flow cytometry. (C) intracellular IFN-γ and IL-17A in Lin$^-$TCR-δ$^+$ thymocytes from *Ptpn2*$^{+/+}$ (C57BL/6) and *Ptpn2*$^{-/-}$ (C57BL/6) mice. (D) Thymocytes from poly (I:C)–treated *Rosa26-eYFP;Ptpn2*$^{fl/fl}$ (C57BL/6) and *Mx1*-Cre;*Rosa26-eYFP;Ptpn2*$^{fl/fl}$ (C57BL/6) mice were stained with α-galactosylceramide–loaded CD1d tetramers (CD1d/α-GC) and α-TCR-β or α-CD4, α-CD25, and intracellular α-FoxP3. CD1d/αGC tetramer$^+$TCR-β$^+$ NKT cells or CD4$^+$CD25$^+$FoxP3$^+$ T reg cells were quantified by flow cytometry. (E) FACS-purified, CTV-labeled Lin$^-$ DN3a thymocytes from *Ptpn2*$^{+/+}$ (C57BL/6) and *Ptpn2*$^{-/-}$ (C57BL/6) mice were cultured on OP9-DL1 stromal cells. Thymocytes were harvested after 96 h and stained for TCR-δ and CD45. CTV dilution and the generation of total and CD45$^+$TCR-δ^{hi} T cells per division were monitored by flow cytometry. (F) CD45$^+$CD3$^+$TCR-δ$^+$ IEL and LP lymphocytes in poly (I:C)–treated *Rosa26-eYFP;Ptpn2*$^{fl/fl}$ (C57BL/6) and *Mx1*-Cre;*Rosa26-eYFP;Ptpn2*$^{fl/fl}$ (C57BL/6) mice were determined by flow cytometry. (G) The levels of intracellular IFN-γ and IL-17A in CD45$^+$TCR-δ^{hi} IELs from poly (I:C)–treated *Rosa26-eYFP;Ptpn2*$^{fl/fl}$ (C57BL/6) and *Mx1*-Cre;*Rosa26-eYFP;Ptpn2*$^{fl/fl}$ (C57BL/6) mice were determined by flow cytometry. (H) Lin$^-$ thymocytes from *Ptpn2*$^{+/+}$ (C57BL/6), *Ptpn2*$^{+/+}$;*Lck*$^{+/-}$ (C57BL/6), *Ptpn2*$^{-/-}$ (C57BL/6), or *Ptpn2*$^{-/-}$;*Lck*$^{+/-}$ (C57BL/6) mice were stained for TCR-δ, and TCR-δ$^+$ cells were quantified by flow cytometry. (I and J) FACS-purified Lin$^-$ DN3a thymocytes from *Ptpn2*$^{+/+}$ (C57BL/6), *Ptpn2*$^{-/-}$ (C57BL/6), and *Ptpn2*$^{-/-}$;*Lck*$^{+/-}$ (C57BL/6) mice (I) or poly (I:C)–treated *Rosa26-YFP;Ptpn2*$^{fl/fl}$ (C57BL/6), *Mx1*-Cre;*Rosa26-eYFP;Ptpn2*$^{fl/fl}$ (C57BL/6), and *Mx1*-Cre;*Rosa26-eYFP;Ptpn2*$^{fl/fl}$;*Stat5*$^{fl/+}$ (C57BL/6) mice (J) were cultured on OP9-DL1 stromal cells for 4 d. Cells were harvested and stained for TCR-δ. TCR-δ$^+$ T cell numbers were determined by flow cytometry. (K) FACS-purified Lin$^-$ DN3a thymocytes from *Ptpn2*$^{+/+}$ (C57BL/6) and *Ptpn2*$^{-/-}$ (C57BL/6) mice were cultured on OP9-DL1 stromal cells in the presence of DMSO vehicle control, the SFK PTK inhibitor SU6656, or the PTK JAK inhibitor CMP6 for 4 d. Cells were harvested and stained for TCR-δ, and TCR-δ$^+$ T cell numbers were quantified by flow cytometry. Representative results (means ± SEM; *Ptpn2*$^{+/+}$, $n = 4–7$; *Ptpn2*$^{-/-}$, $n = 4–8$; *Ptpn2*$^{+/+}$;*Lck*$^{+/-}$, $n = 6$; *Ptpn2*$^{-/-}$;*Lck*$^{+/-}$, $n = 5–6$; *Rosa26-eYFP;Ptpn2*$^{fl/fl}$, $n = 4–6$; *Mx1*-Cre;*Rosa26-eYFP;Ptpn2*$^{fl/fl}$, $n = 4–6$; and *Mx1*-Cre;*Rosa26-eYFP;Ptpn2*$^{fl/fl}$;*STAT5*$^{fl/+}$, $n = 5$) and representative cytometry profiles (A, F, and G) from at least two (D and H–K) or three (A–C and E–G) independent experiments are shown. Significance was determined using two-tailed Mann-Whitney *U* test. *, $P < 0.05$; **, $P < 0.01$; ***, $P < 0.001$.

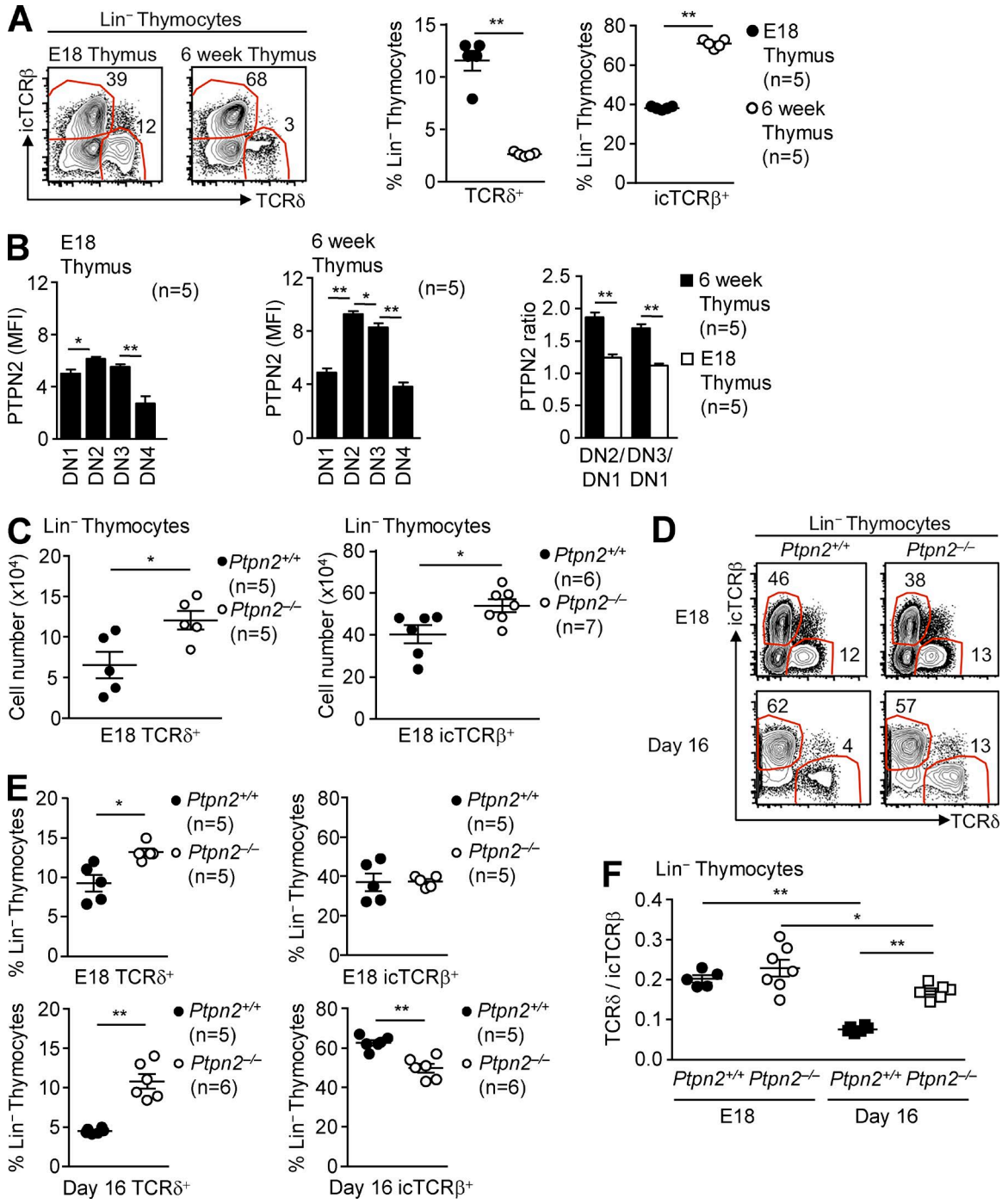

Figure 10. **A postnatal increase in PTPN2 attenuates γδ TCR T cell development.** (A) Lin⁻ thymocytes from E18 and 6-wk-old C57BL/6 mice were stained for TCR-δ and intracellular TCR-β (icTCRβ⁺). The proportions of TCR-δ⁺ and TCR-β⁺ thymocytes were determined by flow cytometry. (B) Lin⁻ thymocytes from E18 and 6-wk-old C57BL/6 mice were stained for CD25, CD44, and intracellular PTPN2. Relative PTPN2 levels (MFI) adjusted to cell size (PTPN2 MFI/FSC), as well as PTPN2 DN2/DN1 and DN3/DN1 ratios in E18 versus 6-wk-old C57BL/6 mice, were determined by flow cytometry. (C) Lin⁻ thymocytes from E18 *Ptpn2*$^{+/+}$ (C57BL/6) and *Ptpn2*$^{-/-}$ (C57BL/6) embryos were stained for TCR-δ and icTCRβ. TCR-δ⁺ and intracellular TCR-β⁺ cells were quantified by flow cytometry. (D–F) Lin⁻ thymocytes from E18 *Ptpn2*$^{+/+}$ (C57BL/6) and *Ptpn2*$^{-/-}$ (C57BL/6) embryos and 16-d-old *Ptpn2*$^{+/+}$ (C57BL/6) and *Ptpn2*$^{-/-}$ (C57BL/6) mice were stained for TCR-δ and icTCRβ. The proportions of TCR-δ⁺ versus intracellular TCR-β⁺ cells (D and E) and TCR-δ⁺/icTCRβ⁺ cell ratios (F) were determined by flow cytometry. Representative results (means ± SEM; C57BL/6, $n = 5$; *Ptpn2*$^{+/+}$, $n = 5–6$; and *Ptpn2*$^{-/-}$, $n = 5–7$) and representative cytometry profiles (A and D) from at least three independent experiments are shown. Significance was determined using two-tailed Mann-Whitney *U* test. *, $P < 0.05$; **, $P < 0.01$.

was increased in the absence of PTPN2, whereas *Stat5* heterozygosity in the context of PTPN2 deficiency not only repressed the increase in DN2a cells in vivo, but also decreased DN2b cell numbers relative to those seen in control animals.

Beyond controlling DN2 expansion/survival and T cell lineage commitment, PTPN2 also influenced β selection. In three different models of PTPN2 deficiency, we found that DN3 cells were increased despite DN2b cells being unaltered in vivo. The ability of PTPN2 deficiency to independently affect DN3 cells and β selection was substantiated in *Lck*-Cre;*Ptpn2*$^{fl/fl}$ mice, where *Ptpn2* deletion occurred after the DN2 stage, and by comparison of co-cultures of purified *Ptpn2*$^{+/+}$ versus *Ptpn2*$^{-/-}$ DN3a cells with OP9-DL1 stromal cells. The increase in DN3 cells caused by PTPN2 deficiency could not be ascribed to increased cellular division/proliferation. Instead, the increase in DN3 cells was likely caused by an increase in their survival as a result of enhanced STAT5- and/or pre-TCR–LCK-driven BCL-2 expression. Several lines of evidence point toward PTPN2 deficiency promoting β selection independent of effects on DN3 cell abundance. First, when purified DN3a cells were co-cultured with OP9-DL1 stromal cells, we found that the relative increase in TCR-β$^+$ thymocyte generation accompanying PTPN2 deficiency exceeded the relative increase in total thymocytes at each cell division. Second, the increase in DN3b cells in *Lck*-Cre;*Ptpn2*$^{fl/fl}$ mice was accompanied by a commensurate decrease in DN3a cells. Third, *Stat5* heterozygosity, or JAK/STAT5 pathway inhibition ex vivo, corrected the increase in DN3/4 cells without repressing the increased generation of TCR-β$^+$ thymocytes. Our results demonstrate that the enhanced αβ TCR T cell generation in PTPN2-deficient mice was specifically caused by the enhanced LCK signaling. *Lck* heterozygosity reduced the increased DN3/4 SFK signaling accompanying PTPN2 deficiency and corrected the increase in TCR-β$^+$ thymocytes and the generation of DP and SP thymocytes and peripheral CD4$^+$ and CD8$^+$ T cells. Therefore, the increased LCK signaling is essential for the enhanced β selection and αβ TCR T cell generation. Could other pathways contribute to the increased β selection? Previous studies have variably implicated IL-7 signaling in β selection, reporting that IL-7 is either dispensable or conversely required for β selection and thereon the expansion and/or differentiation of DN3b and DN4 cells (Trigueros et al., 2003; Van De Wiele et al., 2004; Yu et al., 2004; Balciunaite et al., 2005; Boudil et al., 2015). In particular, a recent study indicates that IL-7 inhibits the differentiation of DN3 and DN4 cells but allows for their greater expansion/self-renewal (Boudil et al., 2015). Although the enhanced STAT5 signaling in *Ptpn2*$^{-/-}$ DN3a cells did not influence the generation of TCR-β$^+$ cells, it is important to note that IL-7 may influence β selection via alternate pathways, including via phosphatidylinositol 3-kinase (PI3K) signaling, which is activated by JAK PTKs in parallel to STAT5 (Pallard et al., 1999). Indeed, the hyperactivation of PI3K signaling accompanying PTEN deficiency has been shown to rescue the defective DN thymocyte development in *Il7*$^{-/-}$ mice (Hagenbeek et al., 2004). Although we did not directly assess the PI3K pathway, PTPN2 deficiency did not affect the activation of JAK-1 and therefore is unlikely to alter PI3K signaling.

Precisely how αβ TCR and γδ TCR T cells develop from common DN3 precursors remains unclear. One favored model is the TCR signal strength model, which dictates that weak TCR signals promote the development of αβ TCR T cells, whereas stronger signals, irrespective of whether they emanate from αβ or γδ TCRs, promote γδ TCR T cell commitment (Haks et al., 2005; Hayes et al., 2005; Kreslavsky et al., 2008; Carpenter and Bosselut, 2010; Turchinovich and Hayday, 2011; Wencker et al., 2014; Zarin et al., 2015). TCR signal strength also influences the maturation of γδ T cells, with stronger TCR signaling favoring IFN-γ$^+$ γδ T cells (Jensen et al., 2008; Ribot et al., 2009; Turchinovich and Hayday, 2011; Prinz et al., 2013; Muñoz-Ruiz et al., 2016). PTPN2 deficiency resulted in a 4.5-fold increase in TCR-δ$^+$ thymocytes and a 9.5-fold increase in IEL γδ T cells in *Mx1*-Cre;*Ptpn2*$^{fl/fl}$ mice. The expansion in IEL γδ TCR T cells was predominated by an increased proportion of IFN-γ$^+$ γδ TCR T cells and a decrease in IL-17$^+$ γδ TCR T cells. Whereas IFN-γ$^+$ γδ TCR T cells can originate from DN2 and DN3 thymocytes, IL-17$^+$ γδ TCR T cells are thought to only develop from DN2 thymocytes (Ciofani et al., 2006; Prinz et al., 2006; Shibata et al., 2014). Given that PTPN2 deficiency resulted in a block in T cell lineage commitment and concomitantly enhanced TCR–SFK signaling in DN3/4 cells, we propose that PTPN2 deficiency increased γδ TCR T cell development and IFN-γ$^+$ γδ TCR T cell generation through the enhancement of DN3 TCR/SFK signaling. Consistent with this, *Lck* heterozygosity in vivo or SFK inhibition in DN3a cells ex vivo partially reduced the increased generation of TCR-δ$^+$ thymocytes associated with PTPN2 deficiency. However, it is important to note that γδ TCR T cell development is also dependent on IL-7/IL-7R-α signaling. The importance of IL-7 signaling in γδ TCR T cell development is underscored by the complete absence of γδ TCR T cells in *Il7*$^{-/-}$ or *Il7ra*$^{-/-}$ mice (Cao et al., 1995; Maki et al., 1996; Moore et al., 1996). This contrasts with the incomplete block in αβ TCR T cell production seen in *Il7*- or *Il7ra*-deficient mice (von Freeden-Jeffry et al., 1995; Maraskovsky et al., 1996). Strikingly, we found that *Stat5* heterozygosity or the inhibition of JAK/STAT5 signaling in purified *Ptpn2*$^{-/-}$ DN3a cells reversed the increased generation of TCR-δ$^+$ thymocytes without altering TCR-β$^+$ thymocyte development. These results indicate the PTPN2 deficiency selectively drives the generation of γδ TCR T cells through the enhancement of DN3 STAT5 signaling, which may then act together with the elevated TCR signaling to promote γδ TCR T cell maturation.

The context in which PTPN2 may affect thymic αβ TCR and γδ TCR T cell development remains to be established. Our studies suggest that postnatal increases in PTPN2 at the DN2/3 stage may repress the generation of γδ TCR T cell subsets that otherwise predominate during embryogen-

esis, but further studies are required to specifically compare the *Ptpn2*$^{-/-}$ γδ TCR T cell repertoire during embryogenesis and postnatal development. Nonetheless, considering that γδ TCR T cell development in *Ptpn2*$^{-/-}$ mice was skewed toward the IFN-γ–producing subsets, it is possible that alterations in PTPN2 may influence γδ TCR T cell–mediated immunity. In human diseases, such as Crohn's disease and ulcerative colitis, γδ TCR T cells have been reported to accumulate in inflamed tissues (McVay et al., 1997; Yeung et al., 2000), and there is increasing evidence that IEL γδ TCR T cell expansion can perturb intestinal homeostasis and contribute to the development of colitis (Mizoguchi et al., 1996; Nanno et al., 2008; Park et al., 2010). *PTPN2* single nucleotide polymorphisms that result in decreased *PTPN2* mRNA and protein levels have been associated with the development of inflammatory bowel disease, in particular Crohn's disease (Wellcome Trust Case Control Consortium, 2007; Festen et al., 2011; Scharl et al., 2012). Although a recent study points toward this being caused by aberrant CD4$^+$ T cell differentiation (Spalinger et al., 2015), it is possible that γδ TCR T cell alterations accompanying PTPN2 deficiency may also exacerbate disease progression.

The results of this study provide insight into the molecular mechanisms by which two critical early T cell developmental checkpoints are regulated. Our findings reveal that PTPN2 is instrumental in the coordination of T cell lineage commitment through the control of STAT5 signaling and αβ TCR versus γδ TCR T cell specification by controlling SFK and STAT5 signaling. This highlights the possibility that alterations in the levels and/or function of PTPN2 at the DN stage of thymocyte differentiation may impact on the T cell repertoire in different physiological or pathological contexts.

MATERIALS AND METHODS

Mice

Mice were maintained on a 12-h light/dark cycle in a temperature-controlled high barrier facility (Animal Research Laboratory, Monash University) with free access to food and water. *Ptpn2*$^{-/-}$ mice backcrossed for eight generations onto a BALB/c background (You-Ten et al., 1997; Wiede et al., 2012) or generated on a C57BL/6 background have been described previously (Wiede et al., 2012). Unless otherwise stated in the figure legend, *Ptpn2*$^{-/-}$ mice used throughout the study were on the C57BL/6 background. C57BL/6J mice were purchased from the Monash Animal Research Platform (MARP; Monash University). C57BL/6.Ly5.1 (B6.SJL-*Ptprc*^{a}*Pepc*^{b}/BoyJ) mice were purchased from The Walter and Eliza Hall Institute of Medical Research Animal Facility and bred with C57BL/6J mice (MARP) to generate C57BL/6.Ly5.1$^+$/2$^+$ mice. BALB/c.Thy1.1 were purchased from MARP and backcrossed for five generations. B6.129X1-*Gt(ROSA)26Sor*$^{tm1(EYFP)Cos}$/J and B6.Cg-Tg(*Mx1*-Cre)1Cgn/J mice were purchased from The Jackson Laboratory and were bred with *Ptpn2*$^{fl/fl}$ (C57BL/6) mice to generate *Mx1*-Cre;*Rosa26-eYFP;Ptpn2*$^{fl/fl}$ mice. *Stat5*$^{fl/fl}$ (C57BL/6) mice have been described previously (Gurzov et al., 2014) and were bred with *Mx1*-Cre;*Rosa26-eYFP;Ptpn2*$^{fl/fl}$ mice to generate *Mx1*-Cre;*Rosa26-eYFP;Ptpn2*$^{fl/fl}$;*Stat5*$^{fl/+}$ mice. B6.129S2-*Lck*<tm1Mak>/J mice were a gift from A. Veillette (McGill University, Montreal, Canada) and were bred with *Ptpn2*$^{+/-}$ mice to generate *Ptpn2*$^{-/-}$;*Lck*$^{+/-}$ mice. For irradiation and adoptive transfer experiments, 6–8-wk-old BALB/c.Thy1.2, C57BL/6.Ly5.1$^+$.Ly5.2$^+$, or C57BL/6.Ly5.2$^+$ female recipient mice were used, and donor mice were 2–8 wk old and sex matched. Age- and sex-matched littermates were used in all experiments.

Materials

The SFK PTK inhibitors Saracatinib (AZD0530) and SU6656 and the JAK PTK inhibitor CMP6 were purchased from Merck Millipore. Recombinant mouse IL-7, murine stem cell factor, IL-3, IL-6, and FLT3L were purchased from Peprotech. Antibodies against STAT5, p-(Y694) STAT5, p-(Y1022/1023) JAK-1, and JAK-1 were purchased from Cell Signaling. Tubulin was purchased from Sigma-Aldrich. Retronectin was purchased from Takara. Poly (I:C), Percoll, and Dnase I were from Sigma-Aldrich; FBS was from Thermo Fisher; Dulbecco-PBS (D-PBS) and HBSS were from Invitrogen; and collagenase D was from Roche. The mouse antibody against PTPN2 (6F3) and plasmid encoding murine PTPN2 (Ptpn2-pcDNA3.1) were provided by M. Tremblay (McGill University).

Flow cytometry

Single-cell thymic suspensions were obtained by gently compressing thymi between two frosted glass slides. Cell suspensions were homogenized further with an 18-gauge needle followed by a wash with ice-cold D-PBS supplemented with 2% (vol/vol) FBS (D-PBS/2% FBS) and incubated for 5 min on ice in red blood cell lysing buffer (Sigma-Aldrich) to remove contaminating erythrocytes. Lymphocyte counts (4–15 µm) were determined with a Z2 Coulter Counter (Beckman Coulter). For surface staining, 10^6/10 µl cells were resuspended in D-PBS/2% FBS containing the antibody cocktail in 96-well microtiter plates (BD Biosciences) for 20 min on ice in the dark. For FACS sorting, cells were stained in 15-ml Falcon tubes (BD Biosciences) for 30 min on ice. Thymocytes were stained with biotinylated antibodies against lineage (Lin) markers (CD4, CD8, CD3, GR-1, B220, CD19, CD11b, CD11c, NK1.1, and TER119; Miltenyi) and fluorochrome-conjugated antibodies against CD25, CD27, CD44, and c-KIT, incubated with fluorochrome-conjugated streptavidin (to label cells stained with the biotinylated antibodies), and analyzed using an LSRII, Fortessa (BD Biosciences), or CyAn advanced digital processing analyzer (Beckman Coulter).

For FACS purification of DN cell subsets, thymocytes were stained with biotinylated antibodies against CD3 (145-2C11), CD4 (RM4-5), and CD8 (53–6.7; BD Biosciences) and then with streptavidin beads (Miltenyi) in D-PBS supple-

mented with 0.5% (wt/vol) BSA. DP and SP thymocytes were then depleted with the autoMACS Separator (Miltenyi). These DP/SP-depleted thymocytes were then incubated with biotinylated antibodies against Lin markers (see above) and fluorochrome-conjugated antibodies against CD25, CD27, CD44, and c-KIT followed by fluorochrome-conjugated streptavidin (to label cells stained with the biotinylated antibodies). DN cell subsets were purified using a cell sorter (Influx; BD Biosciences). FACS-purified DN1 ($Lin^-CD25^-CD44^+c\text{-}KIT^{hi}$), DN2a ($Lin^-CD25^+CD44^+c\text{-}KIT^{hi}$), and DN3a ($Lin^-CD25^+CD27^-CD44^-c\text{-}KIT^-$) cells or FACS-purified $Lin^-SCA\text{-}1^+c\text{-}KIT^+$ hematopoietic stem cells isolated from WBM were routinely tested for purity (>99%). Lymphocytes were gated for $eYFP^+$ cells to discriminate between PTPN2-positive and PTPN2-negative cells after poly (I:C)–induced *Ptpn2* deletion in *Mx1*-Cre;*Rosa26-eYFP;Ptpn2*$^{fl/fl}$ mice. Data were analyzed using FlowJo8.7 or FlowJo10 (Tree Star Inc.) software. For cell quantification, a known number of Calibrite beads (BD Biosciences) or Nile red beads (Prositech) were added to samples before analysis.

The following antibodies from BD PharMingen, BioLegend, or eBioscience were used for flow cytometry: FITC or V450-conjugated CD44 (IM7); PE–cyanine 7 (PE-Cy7)–conjugated or Pacific blue (PB)–conjugated CD69 (H1.2F3); PE-conjugated CD3 (145-2C11); allophycocyanin (APC)-Cy7–conjugated TCR-β (H57-597); PE–cyanine 5 (PE-Cy5)–conjugated, BD Horizon V421–conjugated, or FITC-conjugated TCR-δ (GL3); PE-Cy7–conjugated CD4 (RM4-5); PB-conjugated or Alexa Fluor 647–conjugated CD8 (53–6.7); Alexa Fluor 647–conjugated CD11c (N418); PE-conjugated or PE-Cy7–conjugated NK1.1 (PK136); FITC-conjugated CD24 (M1/69); FITC-, PE-, or APC-Cy7–conjugated CD25 (PC61); PE-Cy7–conjugated CD27 (LG.7F9); APC-conjugated CD45 (30-F11); PE-conjugated CD45.1 (A20); PB-conjugated CD45.2 (104); FITC-conjugated CD90.2 (53–2.1); PE-conjugated CD122 (TM-β1); PE-conjugated CD127 (SB/199); PE-conjugated CD132 (4G3); PE-, APC-, or PerCP-Cy5.5–conjugated c-KIT (2B8); PE-Cy7–conjugated SCA-1 (D7); FITC- or BD Horizon V421–conjugated IL-17A (TC11-18H10.1); PE- or PE-Cy7–conjugated IFN-γ (XMG1.2); Alexa Fluor 647–conjugated BCL-2 (10C4); PE-Cy7–conjugated Ki67 (SolA15); PB-conjugated FoxP3 (MF23); and eFluor 660–conjugated p-(Y418) Src (SC1T2M3). APC-, PE-Cy7–conjugated, or BD Horizon V500–conjugated streptavidin was used to detect cells stained with biotinylated antibodies. APC-labeled α-galactosylceramide (α-GalCer)–loaded CD1 tetramers were produced in house.

Intracellular staining for flow cytometry

3×10^6 freshly isolated thymocytes were stained with biotinylated antibodies against Lin markers followed by incubation with fluorochrome-conjugated streptavidin and fixation in 300 µl Cytofix fixation buffer (BD Biosciences) for 15 min at 37°C. Cells were washed twice with D-PBS to remove excess paraformaldehyde and were permeabilized in 300 µl methanol/acetone (50:50) for 30 min on ice or overnight at −20°C. Permeabilized cells were washed three times with D-PBS/5% (vol/vol) FBS and processed for intracellular staining for PTPN2 (6F3) or p-STAT5 (Y694) (D47E7 XP rabbit; Cell Signaling) in D-PBS/5% (vol/vol) FBS for 1 h at room temperature. Secondary antibodies against mouse IgG (H+L) F(ab′)2 fragment conjugated to FITC or Alexa Fluor 647 (Molecular Probes/Invitrogen) and antibodies against rabbit IgG (H+L) F(ab′)2 fragment coupled to DyLight 649 (Jackson ImmunoResearch) were used for staining for PTPN2 and p-(Y694) STAT5, respectively.

For detection of intracellular TCR-β, Ki67, BCL-2, or FoxP3, the Foxp3/Transcription Factor Staining Buffer set (eBioscience) was used according to the manufacturer's instructions. For the detection of intracellular cytokines, cells were stimulated with the cell stimulation cocktail (plus protein transport inhibitors; eBioscience) for 4 h in complete T cell medium at 37°C. Cells were harvested, fixed, and permeabilized with the BD Cytofix/Cytoperm kit according to the manufacturer's instructions. Cells were stained with the specified antibodies at room temperature for 30 min and processed for flow cytometry.

Thymocyte culture on OP9-DL1 stromal cells

2×10^5 OP9-DL1 cells were seeded in 6-well dishes in complete MEM (supplemented with 10% (vol/vol) FBS, 2 mM L-glutamine, 100 U/ml penicillin/100 µg/ml streptomycin, nonessential amino acids, 1 mM sodium-pyruvate, 10 mM Hepes, 50 µM 2-mercaptoethanol, 1 ng/ml IL-7, and 5 ng/ml FLT3L). 2×10^5 WBM cells or 5×10^4 FACS-purified $Lin^-SCA\text{-}1^+c\text{-}KIT^+$ hematopoietic stem cells isolated from WBM were added and incubated at 37°C for 5 d. At day 5, differentiated DN thymocytes were harvested and filtered through a 100 µM cell strainer to remove OP9-DL1 stromal cells. 2×10^5 DN cells were replated on a 6-well dish seeded with 2×10^5 OP9-DL1 stromal cells in complete MEM. At the indicated times, cells were harvested and stained with biotinylated antibodies against Lin markers, fluorochrome-conjugated antibodies against CD25 and CD44, and then fluorochrome-conjugated streptavidin (to label cells stained with biotinylated antibodies) and finally analyzed by flow cytometry.

For the assessment of DN2a thymocyte differentiation, freshly isolated $Lin^-c\text{-}KIT^{hi}CD44^{hi}CD25^{hi}$ DN2a thymocytes were first bulk sorted on two-drop enrichment mode with the Influx sorter. Enriched DN2a cells were sorted into flat-bottom 96-well plates on single cell sort mode (Influx sorter) seeded with 2.5×10^3 OP9-DL1 stromal cells in complete MEM. At day 3, cells were harvested and stained with fluorochrome-conjugated antibodies against CD25 and c-KIT and then analyzed by flow cytometry. For quantification of the DN2a and DN2b cells, Nile red beads were added to samples before analysis.

To assess the impact of SFK PTK inhibition on the DN3a to DN4 cell transition, FACS-purified $Lin^-c\text{-}KIT^{lo}$

$CD44^{lo}CD25^{hi}CD27^{lo}$ DN3a cells (3×10^3) from *Rosa26-YFP; Ptpn2*$^{fl/fl}$ (C57BL/6) and *Lck*-Cre;*Rosa26-YFP;Ptpn2*$^{fl/fl}$ (C57BL/6) mice were added to OP9-DL1 stromal cells (5×10^4/well in a 24-well dish) and incubated at 37°C for 2–3 d in the presence of vehicle (DMSO), 400 nM Saracatinib, or 200 nM SU6566. At the indicated times, cells were harvested and stained with fluorochrome-conjugated antibodies against CD25, CD44, CD4, and CD8 and finally analyzed by flow cytometry.

To assess the impact of SFK versus JAK PTK inhibition on the generation of TCR-δ^+ and TCR-β^+ thymocytes in vitro, FACS-purified Lin^-c-$KIT^{lo}CD44^{lo}CD25^{hi}CD27^{lo}$ DN3a cells (10^4) were added to OP9-DL1 stromal cells (2×10^3/well in a 96-well dish) and incubated at 37°C for 4 d in the presence of vehicle (DMSO), 200 nM SU6566, and 100 nM CMP6. At the indicated times, cells were harvested and stained with fluorochrome-conjugated antibodies against TCR-β and TCR-δ and finally analyzed by flow cytometry.

To assess the impact of SFK versus JAK PTK inhibition on DN2a differentiation in vitro, FACS-purified Lin^-c-$KIT^{hi}CD44^{hi}CD25^{hi}$ DN2a cells (2×10^2) were added to OP9-DL1 stromal cells (2×10^3/well in a 96-well dish) and incubated at 37°C for 3 d in the presence of vehicle (DMSO), 400 nM Saracatinib, 200 nM SU6566, and 100 nM CMP6. At the indicated times, cells were harvested and stained with biotinylated antibodies against Lin markers, fluorochrome-conjugated antibodies against CD25, CD44, and c-KIT, and then fluorochrome-conjugated streptavidin and finally analyzed by flow cytometry.

Thymocyte culture on OP9 stromal cells

For the assessment of the generation of $NK1.1^+$ NK cells and $CD11^+$ dendritic cells, FACS-purified Lin^-c-$KIT^{hi}CD44^{hi}CD25^{hi}$ DN2a thymocytes (10^2) were added to OP9 stromal cells (2×10^3/well in a 96-well dish) and incubated at 37°C for 5 d in the presence of 1 ng/ml IL-7 and 5 ng/ml FLT3L in complete MEM. To assess the impact of SFK PTK inhibition versus JAK PTK inhibition, 2×10^2 DN2a thymocytes were incubated in the presence of vehicle (DMSO), 400 nM saracatinib, 200 nM SU6566, and 100 nM CMP6. Cells were harvested and stained with biotinylated antibodies against Lin markers, fluorochrome-conjugated antibodies against NK1.1 and CD11c, and then fluorochrome-conjugated streptavidin and analyzed by flow cytometry.

Assessment of DN3a cell proliferation ex vivo

For the assessment of thymocyte proliferation by CTV (Invitrogen/Molecular Probes) dilution, freshly isolated thymocytes were incubated with CTV in D-PBS supplemented with 0.1% (wt/vol) BSA at a final concentration of 5 μM for 15 min at 37°C. Cells were then washed three times with D-PBS supplemented with 10% (vol/vol) FBS. Lin^-c-$KIT^{lo}CD44^{lo}CD25^{hi}CD27^{lo}CTV^+$ DN3a thymocytes were first bulk sorted on two-drop enrichment mode with the Influx sorter. 5×10^3 enriched DN3a cells were further sorted into flat-bottom 96-well plates seeded with 2.5×10^3 OP9-DL1 stromal cells in complete MEM. At various time points, proliferating cells were harvested and stained with fluorochrome-conjugated antibodies against CD45, TCR-δ, and TCR-β. CTV dilution and the generation of TCR-δ^+ and TCR-β^+ T cells were monitored by flow cytometry. For cell quantification, Nile red beads were added to samples before analysis.

BM chimeras

WBM cells were isolated by flushing the tibias and femurs from 6–8-wk-old mice with ice-cold DMEM supplemented with 10% FBS using a 26-gauge needle. Cells were then gently dissociated using a 22-gauge needle and filtered through a 40-μm cell strainer. Cell suspensions were recovered by centrifugation (300 *g* for 5 min at 4°C), and red blood cells were removed with red blood cell lysis buffer (Sigma-Aldrich). Recipient C57BL/6.Ly5.1/Ly5.2^+ or BALB/c.Thy1.2^+ mice were lethally irradiated with two split doses of 550 cGy total body irradiation (^{137}Cs source) separated by 4 h. 1 d after the final irradiation, 200 μl, comprising 4×10^6 total WBM cells, was injected into the tail vein of recipient mice. Recipients received antibiotics (Baytril; Bayer) in their drinking water for 2 wk after irradiation.

Retroviral plasmids

MSCV-PTPN2 was generated by PCR using Platinum *Pfx* DNA Polymerase (Invitrogen) and *Ptpn2*-pcDNA3.1 as a template. For cloning murine *Ptpn2* cDNA into MSCV-IRES-mCherry (Addgene), the oligonucleotides incorporated a BamH1 site immediately 5′ to the initiation codon and a XhoI site immediately 3′ to the terminating codon. MSCV-PTPN2-R222M was generated by site-directed mutagenesis using *Ptpn2*-pcDNA3.1 as a template before PCR amplification and cloning into the BamH1–XhoI sites in MSCV-IRES-Cherry. MSCV-GFP-PTPN2 was generated by PCR amplifying *Ptpn2*, cloning into the BglII–EcoRI sites of pEGFP-C1 (Clontech), and then PCR amplifying the *GFP-Ptpn2* cDNA using *Ptpn2*-pEGFP-C1 as a template and cloning into the BamH1–XhoI sites in MSCV-IRES-Cherry. The fidelity of all constructs was confirmed by sequencing.

Retroviral BM cell transduction

2×10^6/ml WBM cells isolated from 6–8-wk-old C57BL/6 mice were incubated with 100 ng/ml murine stem cell factor, 20 ng/ml IL-3, and 50 ng/ml IL-6 in DMEM supplemented with 20% (vol/vol) FBS, 100 U/ml penicillin/100 μg/ml streptomycin, 2 mM L-glutamine, and 50 μM 2-mercaptoethanol for 48 h at 37°C. WBM cells were harvested and spun down onto 15 μg/ml retronectin-coated 12-well plates containing MSCV-IRES-mCherry control retrovirus or MSCV-PTPN2, MSCV-PTPN2-GFP, or MSCV-PTPN2-R222M retroviruses generated using Phoenix packaging cells transfected with the corresponding retroviral plasmids and incubated overnight. WBM cells were harvested, and a second viral transduction was performed. At

48 h after the last transduction, WBM cells were harvested and FACS purified for mCherry$^+$ (MSCV, MSCV-PTPN2 and MSCV-PTPN2-R222M) or mCherry$^+$GFP$^+$ (MSCV-PTPN2-GFP) cells (5×10^5), which were injected together with 5×10^5 WT WBM cells into the tail vein of lethally irradiated C57BL/6 mice.

Isolation of intraepithelial and LP lymphocytes

For the isolation of IELs, the cecum was cut into 0.5–1-cm pieces, which were incubated twice with agitation (250 rpm) in Ca^{2+}- and Mg^{2+}-free HBSS supplemented with 5% (vol/vol) FBS, 2 mM EDTA, 1 mM DTT, and 10 mM Hepes for 15 min at 37°C. Intestinal pieces were filtered with a 100 µM cell strainer, and the flow-through containing the intraepithelial cell fraction was washed twice with DMEM supplemented with 10% (vol/vol) FBS. Intestinal pieces were further digested with agitation (250 rpm) in Ca^{2+} and Mg^{2+} containing HBSS supplemented with 5% (vol/vol) FBS, 1.5 mg/ml collagenase D, and 0.02 mg/ml DNase I for 1 h at 37°C to extract LP lymphocytes. LP lymphocytes were subsequently enriched with a two-layer Percoll gradient at 40 and 80% (vol/vol) in DMEM supplemented with 10% (vol/vol) FBS.

Real-time PCR

RNA was extracted with TRIzol reagent (Invitrogen), and RNA quality and quantity were determined using a fluorospectrometer (NanoDrop 3300; Thermo Fisher). mRNA was reverse transcribed using a High-Capacity cDNA Reverse Transcription kit (Applied Biosystems) and processed for quantitative real-time PCR using the TaqMan Universal PCR Master mix. *Bcl11b* (Mm00480516_m1) gene expression was determined using TaqMan Gene Expression assays (Applied Biosystems) and normalized to *Gapdh* (Mm99999915_g1). Relative quantification was achieved using the ΔΔCt method.

Poly (I:C) treatment

Rosa26-YFP;Ptpn2$^{fl/fl}$ and *Mx1*-Cre;*Rosa26-eYFP;Ptpn2*$^{fl/fl}$ mice were injected intraperitoneally three times with 250 µg poly (I:C) in D-PBS every other day. 4 wk after the last poly (I:C) injection, mice were processed for experiments.

Statistical analyses

Statistical analyses were performed with Prism software (GraphPad) using the nonparametric two-tailed Mann-Whitney *U* test. $P < 0.05$ was considered to be significant.

Animal ethics

All experiments were performed in accordance with the National Health and Medical Research Council (NHMRC) Australian Code of Practice for the Care and Use of Animals. All protocols were approved by the Monash University School of Biomedical Sciences Animal Ethics Committee (ethics numbers MARP/2012/124 and MARP/2014/100).

Online supplemental material

Fig. S1 shows gating strategies for DN thymocyte subsets. Fig. S2 shows PTPN2 protein levels after inducible PTPN2 deletion in DN thymocytes. Fig. S3 shows the effects of PTPN2 deficiency on the generation of DN thymocyte subsets and DP, CD4$^+$, and CD8$^+$ cells in vivo and ex vivo. Fig. S4 shows the impact of PTPN2 deficiency on STAT5 signaling and DN thymocyte survival. Fig. S5 shows the effects of PTPN2 deficiency on SFK signaling and changes in PTPN2 protein levels in DN thymocytes isolated from E16 embryos and mature mice.

ACKNOWLEDGMENTS

We thank Faruk Sacirbegovic for technical support.

This work was supported by the NHMRC of Australia (grant 1013667 to D.I. Godfrey, grant 1016701 to A. Strasser, and grant 1047055 to T. Tiganis) and the Cancer Council Victoria (grant 1106291 to A. Strasser and grant 1106477 to F. Wiede). D.I. Godfrey and A. Strasser are NHMRC Senior Principal Research Fellows (grants 1020770 and1020363, respectively), and T. Tiganis is an NHMRC Principal Research Fellow (grant 1103037). J.A. Dudakov was supported by the National Institutes of Health (grant R00-CA176376), the Cuyamaca Foundation, the Bezos Family Foundation, and the Mechtild Harf Award from the Deutsche Knochenmarkspenderdatei Foundation for Giving Life.

The authors declare no competing financial interests.

Submitted: 10 November 2016

Revised: 26 May 2017

Accepted: 28 June 2017

REFERENCES

Akashi, K., M. Kondo, U. von Freeden-Jeffry, R. Murray, and I.L. Weissman. 1997. Bcl-2 rescues T lymphopoiesis in interleukin-7 receptor-deficient mice. *Cell*. 89:1033–1041. http://dx.doi.org/10.1016/S0092-8674(00)80291-3

Balciunaite, G., R. Ceredig, H.J. Fehling, J.C. Zúñiga-Pflücker, and A.G. Rolink. 2005. The role of Notch and IL-7 signaling in early thymocyte proliferation and differentiation. *Eur. J. Immunol.* 35:1292–1300. http://dx.doi.org/10.1002/eji.200425822

Boudil, A., I.R. Matei, H.Y. Shih, G. Bogdanoski, J.S. Yuan, S.G. Chang, B. Montpellier, P.E. Kowalski, V. Voisin, S. Bashir, et al. 2015. IL-7 coordinates proliferation, differentiation and *Tcra* recombination during thymocyte β-selection. *Nat. Immunol.* 16:397–405. http://dx.doi.org/10.1038/ni.3122

Bourdeau, A., S. Trop, K.M. Doody, D.J. Dumont, and M.L. Tremblay. 2013. Inhibition of T cell protein tyrosine phosphatase enhances interleukin-18-dependent hematopoietic stem cell expansion. *Stem Cells.* 31:293–304. http://dx.doi.org/10.1002/stem.1276

Byth, K.F., L.A. Conroy, S. Howlett, A.J. Smith, J. May, D.R. Alexander, and N. Holmes. 1996. CD45-null transgenic mice reveal a positive regulatory role for CD45 in early thymocyte development, in the selection of CD4+CD8+ thymocytes, and B cell maturation. *J. Exp. Med.* 183:1707–1718. http://dx.doi.org/10.1084/jem.183.4.1707

Campbell, K.J., D.H. Gray, N. Anstee, A. Strasser, and S. Cory. 2012. Elevated Mcl-1 inhibits thymocyte apoptosis and alters thymic selection. *Cell Death Differ.* 19:1962–1971. http://dx.doi.org/10.1038/cdd.2012.84

Cao, X., E.W. Shores, J. Hu-Li, M.R. Anver, B.L. Kelsall, S.M. Russell, J. Drago, M. Noguchi, A. Grinberg, E.T. Bloom, et al. 1995. Defective lymphoid development in mice lacking expression of the common

cytokine receptor γ chain. *Immunity.* 2:223–238. http://dx.doi.org/10.1016/1074-7613(95)90047-0

Carpenter, A.C., and R. Bosselut. 2010. Decision checkpoints in the thymus. *Nat. Immunol.* 11:666–673. http://dx.doi.org/10.1038/ni.1887

Cheng, A.M., I. Negishi, S.J. Anderson, A.C. Chan, J. Bolen, D.Y. Loh, and T. Pawson. 1997. The Syk and ZAP-70 SH2-containing tyrosine kinases are implicated in pre-T cell receptor signaling. *Proc. Natl. Acad. Sci. USA.* 94:9797–9801. http://dx.doi.org/10.1073/pnas.94.18.9797

Chien, Y.H., C. Meyer, and M. Bonneville. 2014. γδ T cells: first line of defense and beyond. *Annu. Rev. Immunol.* 32:121–155. http://dx.doi.org/10.1146/annurev-immunol-032713-120216

Ciofani, M., G.C. Knowles, D.L. Wiest, H. von Boehmer, and J.C. Zúñiga-Pflücker. 2006. Stage-specific and differential notch dependency at the αγ and γδ T lineage bifurcation. *Immunity.* 25:105–116. http://dx.doi.org/10.1016/j.immuni.2006.05.010

Cui, Y., A. Hosui, R. Sun, K. Shen, O. Gavrilova, W. Chen, M.C. Cam, B. Gao, G.W. Robinson, and L. Hennighausen. 2007. Loss of signal transducer and activator of transcription 5 leads to hepatosteatosis and impaired liver regeneration. *Hepatology.* 46:504–513. http://dx.doi.org/10.1002/hep.21713

Fahl, S.P., F. Coffey, and D.L. Wiest. 2014. Origins of γδ T cell effector subsets: a riddle wrapped in an enigma. *J. Immunol.* 193:4289–4294. http://dx.doi.org/10.4049/jimmunol.1401813

Festen, E.A., P. Goyette, T. Green, G. Boucher, C. Beauchamp, G. Trynka, P.C. Dubois, C. Lagacé, P.C. Stokkers, D.W. Hommes, et al. 2011. A meta-analysis of genome-wide association scans identifies IL18RAP, PTPN2, TAGAP, and PUS10 as shared risk loci for Crohn's disease and celiac disease. *PLoS Genet.* 7:e1001283. http://dx.doi.org/10.1371/journal.pgen.1001283

Fukushima, A., K. Loh, S. Galic, B. Fam, B. Shields, F. Wiede, M.L. Tremblay, M.J. Watt, S. Andrikopoulos, and T. Tiganis. 2010. T-cell protein tyrosine phosphatase attenuates STAT3 and insulin signaling in the liver to regulate gluconeogenesis. *Diabetes.* 59:1906–1914. http://dx.doi.org/10.2337/db09-1365

Godfrey, D.I., J. Kennedy, T. Suda, and A. Zlotnik. 1993. A developmental pathway involving four phenotypically and functionally distinct subsets of CD3-CD4-CD8- triple-negative adult mouse thymocytes defined by CD44 and CD25 expression. *J. Immunol.* 150:4244–4252.

Godfrey, D.I., S. Stankovic, and A.G. Baxter. 2010. Raising the NKT cell family. *Nat. Immunol.* 11:197–206. http://dx.doi.org/10.1038/ni.1841

Groves, T., P. Smiley, M.P. Cooke, K. Forbush, R.M. Perlmutter, and C.J. Guidos. 1996. Fyn can partially substitute for Lck in T lymphocyte development. *Immunity.* 5:417–428. http://dx.doi.org/10.1016/S1074-7613(00)80498-7

Gu, H., J.D. Marth, P.C. Orban, H. Mossmann, and K. Rajewsky. 1994. Deletion of a DNA polymerase beta gene segment in T cells using cell type-specific gene targeting. *Science.* 265:103–106. http://dx.doi.org/10.1126/science.8016642

Gurzov, E.N., M. Tran, M.A. Fernandez-Rojo, T.L. Merry, X. Zhang, Y. Xu, A. Fukushima, M.J. Waters, M.J. Watt, S. Andrikopoulos, et al. 2014. Hepatic oxidative stress promotes insulin-STAT-5 signaling and obesity by inactivating protein tyrosine phosphatase N2. *Cell Metab.* 20:85–102. http://dx.doi.org/10.1016/j.cmet.2014.05.011

Hagenbeek, T.J., M. Naspetti, F. Malergue, F. Garçon, J.A. Nunès, K.B. Cleutjens, J. Trapman, P. Krimpenfort, and H. Spits. 2004. The loss of PTEN allows TCR αβ lineage thymocytes to bypass IL-7 and Pre-TCR-mediated signaling. *J. Exp. Med.* 200:883–894. http://dx.doi.org/10.1084/jem.20040495

Haks, M.C., J.M. Lefebvre, J.P. Lauritsen, M. Carleton, M. Rhodes, T. Miyazaki, D.J. Kappes, and D.L. Wiest. 2005. Attenuation of γδTCR signaling efficiently diverts thymocytes to the αβ lineage. *Immunity.* 22:595–606. http://dx.doi.org/10.1016/j.immuni.2005.04.003

Hayday, A.C., H. Saito, S.D. Gillies, D.M. Kranz, G. Tanigawa, H.N. Eisen, and S. Tonegawa. 1985. Structure, organization, and somatic rearrangement of T cell gamma genes. *Cell.* 40:259–269. http://dx.doi.org/10.1016/0092-8674(85)90140-0

Hayes, S.M., L. Li, and P.E. Love. 2005. TCR signal strength influences αβ/γδ lineage fate. *Immunity.* 22:583–593. http://dx.doi.org/10.1016/j.immuni.2005.03.014

Hennet, T., F.K. Hagen, L.A. Tabak, and J.D. Marth. 1995. T-cell-specific deletion of a polypeptide N-acetylgalactosaminyl-transferase gene by site-directed recombination. *Proc. Natl. Acad. Sci. USA.* 92:12070–12074. http://dx.doi.org/10.1073/pnas.92.26.12070

Ikawa, T., S. Hirose, K. Masuda, K. Kakugawa, R. Satoh, A. Shibano-Satoh, R. Kominami, Y. Katsura, and H. Kawamoto. 2010. An essential developmental checkpoint for production of the T cell lineage. *Science.* 329:93–96. http://dx.doi.org/10.1126/science.1188995

Iwashima, M., B.A. Irving, N.S. van Oers, A.C. Chan, and A. Weiss. 1994. Sequential interactions of the TCR with two distinct cytoplasmic tyrosine kinases. *Science.* 263:1136–1139. http://dx.doi.org/10.1126/science.7509083

Jensen, K.D., X. Su, S. Shin, L. Li, S. Youssef, S. Yamasaki, L. Steinman, T. Saito, R.M. Locksley, M.M. Davis, et al. 2008. Thymic selection determines γδ T cell effector fate: antigen-naive cells make interleukin-17 and antigen-experienced cells make interferon γ. *Immunity.* 29:90–100. http://dx.doi.org/10.1016/j.immuni.2008.04.022

Kang, J., M. Coles, and D.H. Raulet. 1999. Defective development of γ/δ T cells in interleukin 7 receptor-deficient mice is due to impaired expression of T cell receptor γ genes. *J. Exp. Med.* 190:973–982. http://dx.doi.org/10.1084/jem.190.7.973

Kang, J., A. Volkmann, and D.H. Raulet. 2001. Evidence that γδ versus αβ T cell fate determination is initiated independently of T cell receptor signaling. *J. Exp. Med.* 193:689–698. http://dx.doi.org/10.1084/jem.193.6.689

Kreslavsky, T., A.I. Garbe, A. Krueger, and H. von Boehmer. 2008. T cell receptor-instructed αβ versus γδ lineage commitment revealed by single-cell analysis. *J. Exp. Med.* 205:1173–1186. http://dx.doi.org/10.1084/jem.20072425

Kueh, H.Y., M.A. Yui, K.K. Ng, S.S. Pease, J.A. Zhang, S.S. Damle, G. Freedman, S. Siu, I.D. Bernstein, M.B. Elowitz, and E.V. Rothenberg. 2016. Asynchronous combinatorial action of four regulatory factors activates Bcl11b for T cell commitment. *Nat. Immunol.* 17:956–965. http://dx.doi.org/10.1038/ni.3514

Kühn, R., F. Schwenk, M. Aguet, and K. Rajewsky. 1995. Inducible gene targeting in mice. *Science.* 269:1427–1429. http://dx.doi.org/10.1126/science.7660125

Lam, M.H., B.J. Michell, M.T. Fodero-Tavoletti, B.E. Kemp, N.K. Tonks, and T. Tiganis. 2001. Cellular stress regulates the nucleocytoplasmic distribution of the protein-tyrosine phosphatase TCPTP. *J. Biol. Chem.* 276:37700–37707. http://dx.doi.org/10.1074/jbc.M105128200

Li, L., M. Leid, and E.V. Rothenberg. 2010a. An early T cell lineage commitment checkpoint dependent on the transcription factor *Bcl11b*. *Science.* 329:89–93. http://dx.doi.org/10.1126/science.1188989

Li, P., S. Burke, J. Wang, X. Chen, M. Ortiz, S.C. Lee, D. Lu, L. Campos, D. Goulding, B.L. Ng, et al. 2010b. Reprogramming of T cells to natural killer-like cells upon *Bcl11b* deletion. *Science.* 329:85–89. http://dx.doi.org/10.1126/science.1188063

Loh, K., A. Fukushima, X. Zhang, S. Galic, D. Briggs, P.J. Enriori, S. Simonds, F. Wiede, A. Reichenbach, C. Hauser, et al. 2011. Elevated hypothalamic TCPTP in obesity contributes to cellular leptin resistance. *Cell Metab.* 14:684–699. http://dx.doi.org/10.1016/j.cmet.2011.09.011

Long, S.A., K. Cerosaletti, J.Y. Wan, J.C. Ho, M. Tatum, S. Wei, H.G. Shilling, and J.H. Buckner. 2011. An autoimmune-associated variant in *PTPN2* reveals an impairment of IL-2R signaling in $CD4^+$ T cells. *Genes Immun.* 12:116–125. http://dx.doi.org/10.1038/gene.2010.54

Maki, K., S. Sunaga, Y. Komagata, Y. Kodaira, A. Mabuchi, H. Karasuyama, K. Yokomuro, J.I. Miyazaki, and K. Ikuta. 1996. Interleukin 7 receptor-deficient mice lack gammadelta T cells. *Proc. Natl. Acad. Sci. USA.* 93:7172–7177. http://dx.doi.org/10.1073/pnas.93.14.7172

Maraskovsky, E., M. Teepe, P.J. Morrissey, S. Braddy, R.E. Miller, D.H. Lynch, and J.J. Peschon. 1996. Impaired survival and proliferation in IL-7 receptor-deficient peripheral T cells. *J. Immunol.* 157:5315–5323.

Maraskovsky, E., L.A. O'Reilly, M. Teepe, L.M. Corcoran, J.J. Peschon, and A. Strasser. 1997. Bcl-2 can rescue T lymphocyte development in interleukin-7 receptor-deficient mice but not in mutant *rag-1*$^{-/-}$ mice. *Cell.* 89:1011–1019. http://dx.doi.org/10.1016/S0092-8674(00)80289-5

McVay, L.D., B. Li, R. Biancaniello, M.A. Creighton, D. Bachwich, G. Lichtenstein, J.L. Rombeau, and S.R. Carding. 1997. Changes in human mucosal gamma delta T cell repertoire and function associated with the disease process in inflammatory bowel disease. *Mol. Med.* 3:183–203.

Mizoguchi, A., E. Mizoguchi, C. Chiba, G.M. Spiekermann, S. Tonegawa, C. Nagler-Anderson, and A.K. Bhan. 1996. Cytokine imbalance and autoantibody production in T cell receptor-alpha mutant mice with inflammatory bowel disease. *J. Exp. Med.* 183:847–856. http://dx.doi.org/10.1084/jem.183.3.847

Molina, T.J., K. Kishihara, D.P. Siderovski, W. van Ewijk, A. Narendran, E. Timms, A. Wakeham, C.J. Paige, K.U. Hartmann, A. Veillette, et al. 1992. Profound block in thymocyte development in mice lacking p56^{lck}. *Nature.* 357:161–164. http://dx.doi.org/10.1038/357161a0

Moore, T.A., U. von Freeden-Jeffry, R. Murray, and A. Zlotnik. 1996. Inhibition of γ δ T cell development and early thymocyte maturation in IL-7 -/- mice. *J. Immunol.* 157:2366–2373.

Muñoz-Ruiz, M., J.C. Ribot, A.R. Grosso, N. Gonçalves-Sousa, A. Pamplona, D.J. Pennington, J.R. Regueiro, E. Fernández-Malavé, and B. Silva-Santos. 2016. TCR signal strength controls thymic differentiation of discrete proinflammatory γδ T cell subsets. *Nat. Immunol.* 17:721–727. http://dx.doi.org/10.1038/ni.3424

Nanno, M., Y. Kanari, T. Naito, N. Inoue, T. Hisamatsu, H. Chinen, K. Sugimoto, Y. Shimomura, H. Yamagishi, T. Shiohara, et al. 2008. Exacerbating role of γδ T cells in chronic colitis of T-cell receptor α mutant mice. *Gastroenterology.* 134:481–490. http://dx.doi.org/10.1053/j.gastro.2007.11.056

Nigg, E.A. 1997. Nucleocytoplasmic transport: signals, mechanisms and regulation. *Nature.* 386:779–787. http://dx.doi.org/10.1038/386779a0

Opferman, J.T., A. Letai, C. Beard, M.D. Sorcinelli, C.C. Ong, and S.J. Korsmeyer. 2003. Development and maintenance of B and T lymphocytes requires antiapoptotic MCL-1. *Nature.* 426:671–676. http://dx.doi.org/10.1038/nature02067

Palacios, E.H., and A. Weiss. 2004. Function of the Src-family kinases, Lck and Fyn, in T-cell development and activation. *Oncogene.* 23:7990–8000. http://dx.doi.org/10.1038/sj.onc.1208074

Pallard, C., A.P. Stegmann, T. van Kleffens, F. Smart, A. Venkitaraman, and H. Spits. 1999. Distinct roles of the phosphatidylinositol 3-kinase and STAT5 pathways in IL-7-mediated development of human thymocyte precursors. *Immunity.* 10:525–535. http://dx.doi.org/10.1016/S1074-7613(00)80052-7

Park, S.G., R. Mathur, M. Long, N. Hosh, L. Hao, M.S. Hayden, and S. Ghosh. 2010. T regulatory cells maintain intestinal homeostasis by suppressing γδ T cells. *Immunity.* 33:791–803. http://dx.doi.org/10.1016/j.immuni.2010.10.014

Porritt, H.E., L.L. Rumfelt, S. Tabrizifard, T.M. Schmitt, J.C. Zúñiga-Pflücker, and H.T. Petrie. 2004. Heterogeneity among DN1 prothymocytes reveals multiple progenitors with different capacities to generate T cell and non-T cell lineages. *Immunity.* 20:735–745. http://dx.doi.org/10.1016/j.immuni.2004.05.004

Prinz, I., A. Sansoni, A. Kissenpfennig, L. Ardouin, M. Malissen, and B. Malissen. 2006. Visualization of the earliest steps of γδT cell development in the adult thymus. *Nat. Immunol.* 7:995–1003. http://dx.doi.org/10.1038/ni1371

Prinz, I., B. Silva-Santos, and D.J. Pennington. 2013. Functional development of γδ T cells. *Eur. J. Immunol.* 43:1988–1994. http://dx.doi.org/10.1002/eji.201343759

Ribot, J.C., A. deBarros, D.J. Pang, J.F. Neves, V. Peperzak, S.J. Roberts, M. Girardi, J. Borst, A.C. Hayday, D.J. Pennington, and B. Silva-Santos. 2009. CD27 is a thymic determinant of the balance between interferon-γ- and interleukin 17-producing γδ T cell subsets. *Nat. Immunol.* 10:427–436. http://dx.doi.org/10.1038/ni.1717

Rothenberg, E.V. 2011. T cell lineage commitment: identity and renunciation. *J. Immunol.* 186:6649–6655. http://dx.doi.org/10.4049/jimmunol.1003703

Scharl, M., K.A. Wojtal, H.M. Becker, A. Fischbeck, P. Frei, J. Arikkat, T. Pesch, S. Kellermeier, D.L. Boone, A. Weber, et al. 2012. Protein tyrosine phosphatase nonreceptor type 2 regulates autophagosome formation in human intestinal cells. *Inflamm. Bowel Dis.* 18:1287–1302. http://dx.doi.org/10.1002/ibd.21891

Schmitt, T.M., and J.C. Zúñiga-Pflücker. 2002. Induction of T cell development from hematopoietic progenitor cells by delta-like-1 in vitro. *Immunity.* 17:749–756. http://dx.doi.org/10.1016/S1074-7613(02)00474-0

Schmitt, T.M., M. Ciofani, H.T. Petrie, and J.C. Zúñiga-Pflücker. 2004. Maintenance of T cell specification and differentiation requires recurrent notch receptor-ligand interactions. *J. Exp. Med.* 200:469–479. http://dx.doi.org/10.1084/jem.20040394

Shi, J., and H.T. Petrie. 2012. Activation kinetics and off-target effects of thymus-initiated cre transgenes. *PLoS One.* 7:e46590. http://dx.doi.org/10.1371/journal.pone.0046590

Shibata, K., H. Yamada, M. Nakamura, S. Hatano, Y. Katsuragi, R. Kominami, and Y. Yoshikai. 2014. IFN-γ-producing and IL-17-producing γδ T cells differentiate at distinct developmental stages in murine fetal thymus. *J. Immunol.* 192:2210–2218. http://dx.doi.org/10.4049/jimmunol.1302145

Simoncic, P.D., A. Lee-Loy, D.L. Barber, M.L. Tremblay, and C.J. McGlade. 2002. The T cell protein tyrosine phosphatase is a negative regulator of Janus family kinases 1 and 3. *Curr. Biol.* 12:446–453. http://dx.doi.org/10.1016/S0960-9822(02)00697-8

Smyth, D.J., V. Plagnol, N.M. Walker, J.D. Cooper, K. Downes, J.H. Yang, J.M. Howson, H. Stevens, R. McManus, C. Wijmenga, et al. 2008. Shared and distinct genetic variants in type 1 diabetes and celiac disease. *N. Engl. J. Med.* 359:2767–2777. http://dx.doi.org/10.1056/NEJMoa0807917

Spalinger, M.R., S. Kasper, C. Chassard, T. Raselli, I. Frey-Wagner, C. Gottier, S. Lang, K. Atrott, S.R. Vavricka, F. Mair, et al. 2015. PTPN2 controls differentiation of CD4$^+$ T cells and limits intestinal inflammation and intestinal dysbiosis. *Mucosal Immunol.* 8:918–929. http://dx.doi.org/10.1038/mi.2014.122

Straus, D.B., and A. Weiss. 1992. Genetic evidence for the involvement of the lck tyrosine kinase in signal transduction through the T cell antigen receptor. *Cell.* 70:585–593. http://dx.doi.org/10.1016/0092-8674(92)90428-F

Taghon, T., M.A. Yui, R. Pant, R.A. Diamond, and E.V. Rothenberg. 2006. Developmental and molecular characterization of emerging β- and γδ-selected pre-T cells in the adult mouse thymus. *Immunity.* 24:53–64. http://dx.doi.org/10.1016/j.immuni.2005.11.012

ten Hoeve, J., M. de Jesus Ibarra-Sanchez, Y. Fu, W. Zhu, M. Tremblay, M. David, and K. Shuai. 2002. Identification of a nuclear Stat1 protein tyrosine phosphatase. *Mol. Cell. Biol.* 22:5662–5668. http://dx.doi.org/10.1128/MCB.22.16.5662-5668.2002

Tiganis, T., and A.M. Bennett. 2007. Protein tyrosine phosphatase function: the substrate perspective. *Biochem. J.* 402:1–15. http://dx.doi.org/10.1042/BJ20061548

Tiganis, T., A.J. Flint, S.A. Adam, and N.K. Tonks. 1997. Association of the T-cell protein tyrosine phosphatase with nuclear import factor p97. *J. Biol. Chem.* 272:21548–21557. http://dx.doi.org/10.1074/jbc.272.34.21548

Todd, J.A., N.M. Walker, J.D. Cooper, D.J. Smyth, K. Downes, V. Plagnol, R. Bailey, S. Nejentsev, S.F. Field, F. Payne, et al. Genetics of Type 1 Diabetes in Finland. Wellcome Trust Case Control Consortium. 2007. Robust associations of four new chromosome regions from genome-wide analyses of type 1 diabetes. *Nat. Genet.* 39:857–864. http://dx.doi.org/10.1038/ng2068

Trigueros, C., K. Hozumi, B. Silva-Santos, L. Bruno, A.C. Hayday, M.J. Owen, and D.J. Pennington. 2003. Pre-TCR signaling regulates IL-7 receptor α expression promoting thymocyte survival at the transition from the double-negative to double-positive stage. *Eur. J. Immunol.* 33:1968–1977. http://dx.doi.org/10.1002/eji.200323831

Turchinovich, G., and A.C. Hayday. 2011. Skint-1 identifies a common molecular mechanism for the development of interferon-γ-secreting versus interleukin-17-secreting γδ T cells. *Immunity.* 35:59–68. http://dx.doi.org/10.1016/j.immuni.2011.04.018

Van De Wiele, C.J.V., J.H. Marino, B.W. Murray, S.S. Vo, M.E. Whetsell, and T.K. Teague. 2004. Thymocytes between the β-selection and positive selection checkpoints are nonresponsive to IL-7 as assessed by STAT-5 phosphorylation. *J. Immunol.* 172:4235–4244. http://dx.doi.org/10.4049/jimmunol.172.7.4235

van Vliet, C., P.E. Bukczynska, M.A. Puryer, C.M. Sadek, B.J. Shields, M.L. Tremblay, and T. Tiganis. 2005. Selective regulation of tumor necrosis factor-induced Erk signaling by Src family kinases and the T cell protein tyrosine phosphatase. *Nat. Immunol.* 6:253–260. http://dx.doi.org/10.1038/ni1169

von Freeden-Jeffry, U., P. Vieira, L.A. Lucian, T. McNeil, S.E. Burdach, and R. Murray. 1995. Lymphopenia in interleukin (IL)-7 gene-deleted mice identifies IL-7 as a nonredundant cytokine. *J. Exp. Med.* 181:1519–1526. http://dx.doi.org/10.1084/jem.181.4.1519

von Freeden-Jeffry, U., N. Solvason, M. Howard, and R. Murray. 1997. The earliest T lineage-committed cells depend on IL-7 for Bcl-2 expression and normal cell cycle progression. *Immunity.* 7:147–154. http://dx.doi.org/10.1016/S1074-7613(00)80517-8

Wakabayashi, Y., H. Watanabe, J. Inoue, N. Takeda, J. Sakata, Y. Mishima, J. Hitomi, T. Yamamoto, M. Utsuyama, O. Niwa, et al. 2003. Bcl11b is required for differentiation and survival of α_βT lymphocytes. *Nat. Immunol.* 4:533–539. http://dx.doi.org/10.1038/ni927

Wellcome Trust Case Control Consortium. 2007. Genome-wide association study of 14,000 cases of seven common diseases and 3,000 shared controls. *Nature.* 447:661–678. http://dx.doi.org/10.1038/nature05911

Wencker, M., G. Turchinovich, R. Di Marco Barros, L. Deban, A. Jandke, A. Cope, and A.C. Hayday. 2014. Innate-like T cells straddle innate and adaptive immunity by altering antigen-receptor responsiveness. *Nat. Immunol.* 15:80–87. http://dx.doi.org/10.1038/ni.2773

Wiede, F., B.J. Shields, S.H. Chew, K. Kyparissoudis, C. van Vliet, S. Galic, M.L. Tremblay, S.M. Russell, D.I. Godfrey, and T. Tiganis. 2011. T cell protein tyrosine phosphatase attenuates T cell signaling to maintain tolerance in mice. *J. Clin. Invest.* 121:4758–4774. http://dx.doi.org/10.1172/JCI59492

Wiede, F., S.H. Chew, C. van Vliet, I.J. Poulton, K. Kyparissoudis, T. Sasmono, K. Loh, M.L. Tremblay, D.I. Godfrey, N.A. Sims, and T. Tiganis. 2012. Strain-dependent differences in bone development, myeloid hyperplasia, morbidity and mortality in ptpn2-deficient mice. *PLoS One.* 7:e36703. http://dx.doi.org/10.1371/journal.pone.0036703

Wiede, F., N.L. La Gruta, and T. Tiganis. 2014a. PTPN2 attenuates T-cell lymphopenia-induced proliferation. *Nat. Commun.* 5:3073. http://dx.doi.org/10.1038/ncomms4073

Wiede, F., A. Ziegler, D. Zehn, and T. Tiganis. 2014b. PTPN2 restrains $CD8^+$ T cell responses after antigen cross-presentation for the maintenance of peripheral tolerance in mice. *J. Autoimmun.* 53:105–114. http://dx.doi.org/10.1016/j.jaut.2014.05.008

Wiede, F., F. Sacirbegovic, Y.A. Leong, D. Yu, and T. Tiganis. 2017. PTPN2-deficiency exacerbates T follicular helper cell and B cell responses and promotes the development of autoimmunity. *J. Autoimmun.* 76:85–100. http://dx.doi.org/10.1016/j.jaut.2016.09.004

Yamasaki, S., E. Ishikawa, M. Sakuma, K. Ogata, K. Sakata-Sogawa, M. Hiroshima, D.L. Wiest, M. Tokunaga, and T. Saito. 2006. Mechanistic basis of pre-T cell receptor-mediated autonomous signaling critical for thymocyte development. *Nat. Immunol.* 7:67–75. http://dx.doi.org/10.1038/ni1290

Yao, Z., Y. Cui, W.T. Watford, J.H. Bream, K. Yamaoka, B.D. Hissong, D. Li, S.K. Durum, Q. Jiang, A. Bhandoola, et al. 2006. Stat5a/b are essential for normal lymphoid development and differentiation. *Proc. Natl. Acad. Sci. USA.* 103:1000–1005. http://dx.doi.org/10.1073/pnas.0507350103

Ye, S.-K., K. Maki, T. Kitamura, S. Sunaga, K. Akashi, J. Domen, I.L. Weissman, T. Honjo, and K. Ikuta. 1999. Induction of germline transcription in the TCRγ locus by Stat5: implications for accessibility control by the IL-7 receptor. *Immunity.* 11:213–223. http://dx.doi.org/10.1016/S1074-7613(00)80096-5

Ye, S.-K., Y. Agata, H.C. Lee, H. Kurooka, T. Kitamura, A. Shimizu, T. Honjo, and K. Ikuta. 2001. The IL-7 receptor controls the accessibility of the TCRγ locus by Stat5 and histone acetylation. *Immunity.* 15:813–823. http://dx.doi.org/10.1016/S1074-7613(01)00230-8

Yeung, M.M., S. Melgar, V. Baranov, A. Oberg, A. Danielsson, S. Hammarström, and M.L. Hammarström. 2000. Characterisation of mucosal lymphoid aggregates in ulcerative colitis: immune cell phenotype and TcR-γδ expression. *Gut.* 47:215–227. http://dx.doi.org/10.1136/gut.47.2.215

Yi, Z., W.W. Lin, L.L. Stunz, and G.A. Bishop. 2014. The adaptor TRAF3 restrains the lineage determination of thymic regulatory T cells by modulating signaling via the receptor for IL-2. *Nat. Immunol.* 15:866–874. http://dx.doi.org/10.1038/ni.2944

You-Ten, K.E., E.S. Muise, A. Itié, E. Michaliszyn, J. Wagner, S. Jothy, W.S. Lapp, and M.L. Tremblay. 1997. Impaired bone marrow microenvironment and immune function in T cell protein tyrosine phosphatase-deficient mice. *J. Exp. Med.* 186:683–693. http://dx.doi.org/10.1084/jem.186.5.683

Yu, Q., B. Erman, J.-H. Park, L. Feigenbaum, and A. Singer. 2004. IL-7 receptor signals inhibit expression of transcription factors TCF-1, LEF-1, and RORγt: impact on thymocyte development. *J. Exp. Med.* 200:797–803. http://dx.doi.org/10.1084/jem.20032183

Yui, M.A., N. Feng, and E.V. Rothenberg. 2010. Fine-scale staging of T cell lineage commitment in adult mouse thymus. *J. Immunol.* 185:284–293. http://dx.doi.org/10.4049/jimmunol.1000679

Zarin, P., E.L. Chen, T.S. In, M.K. Anderson, and J.C. Zúñiga-Pflücker. 2015. Gamma delta T-cell differentiation and effector function programming, TCR signal strength, when and how much? *Cell. Immunol.* 296:70–75. http://dx.doi.org/10.1016/j.cellimm.2015.03.007

Zhang, J.A., A. Mortazavi, B.A. Williams, B.J. Wold, and E.V. Rothenberg. 2012. Dynamic transformations of genome-wide epigenetic marking and transcriptional control establish T cell identity. *Cell.* 149:467–482. http://dx.doi.org/10.1016/j.cell.2012.01.056